C.P. No. 479
(21,388)
A.R.C. Technical Report

C.P. No. 479
(21,388)
A.R.C. Technical Report

MINISTRY OF AVIATION

AERONAUTICAL RESEARCH COUNCIL

CURRENT PAPERS

Measurements of the Effect of Surface Cooling on Boundary Layer Transition on a 15 Degree Cone

Part II

Tests at M = 3 and M = 4 in the 5 in. x 5 in. No.5 Wind Tunnel at R.A.E. Farnborough

by

J. G. Woodley, M.A.

LONDON: HER MAJESTY'S STATIONERY OFFICE

1960

PRICE 5s. 6d. NET

C.P. No. 479

U.D.C. No. 532.526.3:533.6.011.5:533.696.4:533.6.011.6

Technical Note No. Aero 2628

June, 1959

ROYAL AIRCRAFT ESTABLISHMENT

MEASUREMENTS OF THE EFFECT OF SURFACE COOLING ON BOUNDARY LAYER TRANSITION ON A 15° CONE

PART II. TESTS AT M = 3 AND M = 4 IN THE 5 IN. × 5 IN. NO.5 WIND TUNNEL AT R.A.E. FARNBOROUGH

by

J. G. Woodley, M.A.

SUMMARY

Tests on a steel cone with an included angle of 15° showed that the increase in transition Reynolds number with surface cooling at zero incidence was greater at a local Mach number (M_1) of 2.93 than at M_1 = 3.48.

When the cone was set at an incidence of +2°, transition on the windward side moved aft with cooling at the lower Mach number at approximately the same rate as was found in the zero incidence tests. However at both Mach numbers, little, if any, movement could be seen on the leeward generator. The range of stagnation pressures available did not allow a study of transition to be made on the windward generator at the higher Mach number.

Simultaneous records of transition position on the top and bottom generators of the cone were obtained for all these tests, using the shadowgraph technique.

LIST OF CONTENTS

LIST OF TABLES

LIST OF ILLUSTRATIONS

1 INTRODUCTION

Surface cooling is an effective means of delaying transition from laminar to turbulent flow. Theoretically this has been demonstrated by showing that surface cooling can retard the onset of instability due to two- and three-dimensional disturbances in the laminar layer[1,2,3].

The theory on two dimensional disturbances[2] deduces, for a prescribed amount of cooling (expressed by the reduction of surface temperature below that for zero convective heat transfer), a "minimum critical Reynolds number" below which all small disturbances are damped out. These critical Reynolds numbers cannot be identified immediately with the transition Reynolds numbers obtained in practice, for the latter are influenced by surface roughness, pressure gradients[4], shock waves, and main stream turbulence level, which are all neglected in the theory. However, they do indicate the surface cooling effect on transition Reynolds number to be expected when the above influences are not predominant. Reference 5 confirms this indication for the local Mach number range $1.5 < M < 2.5$, which is the region where the theory predicts cooling to be most effective.

The present series of tests were devised to measure surface cooling effect on the transition Reynolds number for local Mach numbers in the range 2 to 4.5. A cone, which has zero pressure gradient along its surface when placed in a uniform supersonic flow field, was taken as the test body. Tests at nominal Mach numbers of 2 and 3 were made in the 8 in. × 9 in. Supersonic Tunnel in the High Speed Laboratory of R.A.E. Bedford, and these are described in Reference 6. The tests reported in the present note are for nominal Mach numbers of 3 (for comparison with the Bedford tests) and 4, and were made in the 5 in. × 5 in. No.5 Supersonic Tunnel at R.A.E. Farnborough. Originally it had been hoped also to make tests at a Mach number of 4.5, but a preliminary test at this Mach number showed that this would be impossible, for with the cone at zero incidence to the airstream, at the maximum stagnation pressure available, the flow was completely laminar even under conditions corresponding to zero convective heat transfer at its surface.

Since small amounts of incidence had been shown in earlier tests[7] to have a very marked effect on transition position, both the Bedford and the present tests were made at incidences of 0° and $+2^\circ$. The shadowgraph technique, which locates roughly the end of the transition "region"[8], was the basic method used for estimating transition position throughout these tests.

2 APPARATUS AND TECHNIQUES

2.1 The No.5 Supersonic Tunnel, R.A.E. Farnborough

This was a continuous non return flow wind tunnel with a 5 in. × 5 in. working section, shown in Figs.1(a) and 1(b). Stagnation pressure could be varied from 1 to 5 atmospheres and held, if necessary, to within $\pm 1/10$ in. of Hg. Stagnation temperature could be held steady to within $\pm 1/10\ ^\circ C$ for values up to $50^\circ C$, which is the upper limit set by the use of wooden liners. The appropriate test conditions for $M = 3$ and $M = 4$ are tabulated below.

/Table

Nominal Mach number M	Mach number in working section ahead of cone M_∞	Mach number outside boundary layer on cone surface M_1	Range of stagnation pressure used (Atmospheres)	Range of stagnation temperature used (°C)	Local Reynolds number per inch. per atmos. corresponding to Stag. Temp. range given
3	3.13	2.93	3 - 5	28 to 35	0.181×10^6 to 0.175×10^6
4	3.8	3.48	3 - 5	38 to 44	0.122×10^6 to 0.118×10^6

Details of the settling chamber, filters, turbulence level, and humidity are given in Appendix 1.

The optical system, seen in Figs.1(a) and 1(b), was basically a standard two-mirror schlieren system having spherical mirrors of eight inches diameter and six feet focal length. In addition to this a cylindrical lens system was constructed, following the method used in Reference 11, whereby the normal schlieren image of the boundary layer could be magnified normal to the surface. This enabled a closer study of the transition region to be made but had the drawback that the boundary layers on the top and bottom generators of the cone could not be observed simultaneously as would be the case for more conventional schlieren systems.

For simultaneous observation of the boundary layer on the top and bottom generators of the cone a simple shadowgraph system was used.

2.2 Models (For full details see Ref.6)

2.2.1 15° static pressure cone (copper)

This is a sharply pointed 15° copper cone nine inches in length, with $\frac{1}{2}$ mm pressure holes spaced along two opposite generators.

2.2.2 15° heat transfer cone (mild steel)

This cone is nine inches long and has a wall thickness of $^1/_{10}$ inch. It is instrumented with mild steel/constantan thermocouples, which use the steel shell as a common return and are spaced mainly along its upper and lower generators.

The wall of the cone is cooled by an internal circulation of cold alcohol, which is fed from a cooling system (fully described in Ref.6) using solid carbon dioxide as a heat extractor.

2.3 Measuring techniques

2.3.1 Test procedure

For tests at zero convective heat transfer the cone was free of coolant and was allowed to warm up to a steady temperature. The constancy of the reading of the thermocouple at station 2.6 T (2.6 inches from the tip along the top generator) was used as a guide for this purpose.

With the stagnation pressure controlled to within ±0.2" of mercury and the stagnation temperature held to within $\pm\frac{1}{4}^{\circ}C$, a complete record of the cone temperature distribution was then made and shadowgraph and magnified schlieren pictures of the transition position were taken.

The technique used for the tests with coolant flowing through the cone was similar to that used for zero heat transfer tests. Here, however, in order to hold the cone wall to a steady temperature, there was the additional requirement that a steady flow of coolant at a fixed temperature had to be maintained whilst the cone thermocouples were being read.

2.3.2 Measurement of stagnation pressure

The stagnation pressure was sampled from a tapping at the top of the settling chamber, and was measured primarily by a Midwood automatic self-balancing capsule manometer[12]. However, since this manometer only had the range 0 to 4 atmospheres absolute, a large mercury filled glass manometer was used in the range 4 to 5 atmospheres absolute. The Midwood manometer had a measuring accuracy of ±0.01 inches of mercury and the glass manometer an accuracy of ±0.05 inches of mercury.

2.3.3 Measurement of stagnation temperature

The stagnation temperature distribution was measured by placing a grid of copper/constantan thermocouples between the two pipes forming the settling chamber. (The position of this grid being clearly seen in Fig.1(a).) The grid had seventeen thermocouples on it, placed to form a cross. These thermocouples were connected, using a switch over system, to the potentiometer used for measuring the e.m.f. outputs of the cone thermocouples.

From preliminary measurements of the distribution of the stagnation temperature in the settling chamber, using this sytem, it was soon discovered that the thermocouple placed at the centre of the cross configuration gave a good average estimate of temperature condition. Therefore, this single thermocouple was used in the main test series to measure the stagnation temperature.

2.3.4 Measurement of thermocouple output

Thermocouple e.m.f. outputs were measured on a Tinsley constant resistance potentiometer and mirror galvanometer, using a near null system with a least count of one microvolt (which is equivalent to $1/50^{\circ}C$ for the steel/constantan thermocouples on the cone and $1/40^{\circ}C$ for the copper/constantan thermocouples in the settling chamber). The "cold junction" used for this system was an electrically heated Sunvic thermostat which maintained a constant temperature of 40°C as measured by a calibrated mercury thermometer.

2.3.5 Measurement of static pressure in the working section and on the 15° static pressure cone

The measurement of the static pressure distributions in the working section and on the 15° static pressure cone was made on a bank of butyl-phthalate manometers, which had a backing screen graduated in tenths of an inch. (One inch of mercury being approximately equal to thirteen inches of butyl phthalate.) A reference absolute pressure for this system was recorded on a mercury manometer graduated in millimeters.

2.3.6 Measurement of transition position

From the experience of earlier tests[6,8], the shadowgraph technique was chosen as the standard method of recording transition in this series. Its chief advantages over other methods are its simplicity and its speed of

operation. In addition to these however it is independent of model surface temperature, (which is not the case for chemical sublimation and oil flow techniques), and unlike a surface pitot does not interfere with the boundary layer. Also it can record transition on both the top and the bottom generators of the cone simultaneously. This property becomes an important factor when one considers the sensitivity of the transition position to small incidence changes on a body of revolution in supersonic flow.

The shadowgraph pictures were taken with a measuring grid of $\frac{1}{4}$ inch spacing superimposed upon them. This enabled transition position on the cone to be measured to $\pm\frac{1}{8}$ inch. (This would correspond to the statement that for the case in these tests in which the Reynolds number per inch had its maximum value the transition Reynolds number was measured to ±0.11 of a million.)

Closer study of the transition region on one generator was made occasionally using the magnified schlieren system described in section 2.1. The same measuring grid was used and a typical picture of transition obtained is shown in Fig.19. This system produced a vertical magnification of the boundary layer of 12:1 and the pictures obtained were far earier to interpret than the corresponding shadowgraph pictures. Transition position was taken on these pictures to be at the point where the boundary layer image starts to thicken appreciably, and this point, as in the shadowgraph case, could be measured to $\pm\frac{1}{8}$ inch. The results obtained however followed the corresponding results from ordinary shadowgraph so closely that they are omitted from the data presented in this note.

3 RESULTS AND DISCUSSION OF TESTS AT ZERO INCIDENCE

For these tests the cones were set at zero incidence relative to the airstream. The correct setting for this was predetermined for each Mach number by spraying the cone with azobenzene (sublimation indicator of transition) and observing the transition patterns produced. This method proved very effective for the M = 3 tests but results obtained later from shadowgraph for the M = 4 tests seem to indicate that for these tests the cone was eventually set at a slight positive incidence to the airstream.

3.1 Mach number distributions along the top and bottom generators of the 15° copper cone

Static pressures were measured on the 15° copper cone and these were combined with the stagnation pressure (a correction at both M = 3 and M = 4 for the small change in the stagnation pressure through the tip shock would be within the experimental accuracy) to give the Mach number distributions shown in Fig.2. Some of the scatter in the results may be due to the poor surface condition of the copper cone in the neighbourhood of the static pressure orifices. Without the use of a better cone model and additional pressure points it was impossible to determine the nature of the pressure gradients present, but the model was sufficiently good to illustrate the magnitudes of the Mach number deviations experienced along the surface of the cone.

Fig.2(a) shows the results for a nominal tunnel Mach number (M_∞) of 3 for a stagnation pressure of 4 atmospheres. Other results for stagnation pressures of 3 and 5 atmospheres at this Mach number show roughly the same basic trends in pressure fluctuation about the assumed representative local Mach number, which was taken to be 2.93, corresponding to a tunnel Mach number of 3.13. Maximum deviation on the top and the bottom generators from this local value is about $2\frac{1}{2}$%. However transition on the steel cone with cooling, as Fig.2(a) shows, occurred only in a region where the deviation of local Mach number from the chosen value was about 1%.

Fig.2(b) shows the results for a nominal tunnel Mach number (M_∞) of 4 for a stagnation pressure of 4 atmospheres, which again is typical of other results obtained at 3 and 5 atmospheres. The copper cone suffered some deterioration after the Mach 3 tests and as a result of this less pressure points were available for these tests. For these results the representative local Mach number assumed was 3.48, corresponding to a tunnel Mach number of 3.8. Maximum deviation on the top and bottom generators from this local value is again about $2\frac{1}{2}\%$, and, as the diagram shows, deviations of this order were in fact experienced in the regions where transition occurred on the steel cone.

3.2 Surface temperature distributions along the top and bottom generators of the 15° mild steel cone

The 15° mild steel cone was used for all the transition tests and Fig.3 illustrates some surface temperature distributions obtained. Short vertical lines through the curves (full lines for the top generator and broken lines for the bottom generator) show the corresponding transition positions indicated by shadowgraph.

Although the distributions of surface temperature in Fig.3 are for $M_\infty = 3.13$ they are typical of the results obtained at $M_\infty = 3.8$ for the range of pressures 3 to 5 atmospheres.

The top-most curves in Figs.3(a) and 3(b) are for zero heat transfer conditions. The upper and lower limits agree well with temperatures which would be expected with temperature recovery factors (r) of 0.855 (laminar) and 0.88 (turbulent), and it is clear from this that transition indicated by the shadowgraph technique is near to the beginning of the fully turbulent region.

In the Bedford tests[6] it was found that it was far better to cool the cone by having coolant flowing from the base to the tip than in the reverse direction, for in the latter case the surface temperature distributions obtained showed very steep temperature gradients in both the laminar and turbulent regions. As a result of using this favourable system most of the temperature distributions obtained are fairly uniform in the laminar region and resemble Fig.3(a) rather than Fig.3(b). Also, as Fig.3 illustrates, the transition position is shown quite well as a peak in the temperature rise along the cone, although an accurate prediction of transition could not be made from this evidence alone.

Stability theories for the laminar boundary layer assume that the surface temperature is uniform and take no account of temperature gradients. For this reason in the later analysis of the transition results (section 3.3), each temperature distribution is used only to estimate a "representative" laminar boundary layer wall temperature, which is then assumed constant up to transition. Due to the uniformity of the temperature in the laminar layer mentioned above the choice of a representative temperature was in most cases very easy. In more difficult cases, where the wall temperature was seen to increase in the laminar region from its value at the 2.6 inch station to a higher value at the transition point this representative temperature was taken at the point midway between the 2.6 inch station and the transition point. However for the worst cases where transition occurred within two inches of the 2.6 inch station (as in the distributions of Fig.3(b)) the value of the wall temperature at the latter station was taken as the representative temperature, since it was felt that the mid-point was so close to transition as to give an unconservative estimate of the wall cooling required to fix the transition position. (All representative temperatures taken are thus seen to be fairly conservative and in fact an error of 3°C made on estimating these temperatures would cause a change of only 0.01 in the ratio T_w/T_{w_o} used later in section 3 and Figs.5, 6, 7, 8, 10, 11.)

3.3 Transition results from shadowgraph pictures

3.3.1 Zero heat transfer conditions

Figs.4(a) and 4(b) give the transition Reynolds numbers, R_{T_o} (based on local flow conditions), on the top and bottom generators of the steel cone under zero heat transfer conditions at $M_\infty = 3.13$ and $M_\infty = 3.8$, over ranges of stagnation pressure.

The $M_\infty = 3.13$ plots show little change in transition Reynolds number on the top generator with increase in stagnation pressure (decreasing distance from the tip), but on the bottom generator the Reynolds number increases from $2\frac{1}{2}$ to 3 million while p_o increases from 2 to 5 atmospheres.

The $M_\infty = 3.48$ plots show that transition occurred later on the bottom than on the top generator, which may be due to the cone being at a positive incidence to the airstream, although as the tests at $+2^o$ incidence (section 4) illustrate this could only have been slight. Apart from this however the transition Reynolds numbers on both the top and bottom generators increase with increasing stagnation pressure (decreasing distance from the tip). The amount of this increase is about $\frac{1}{2}$ million as the stagnation pressure varies from 3 to 5 atmospheres.

The Bedford tests at $M = 3$ showed this same feature with an increase of 1 million in transition Reynolds number for the stagnation pressure rise from 2 to 4 atmospheres. The reason for this increase is hard to adduce from the present results, but a contributory cause could be non uniformities of the flow in the working section (Fig.2). An effect of tip thickness on the Reynolds number per inch along the cone surface can be ruled out, for the maximum Reynolds numbers based on tip radius for the results at $M = 3$ and $M = 4$ were only respectively of the orders 300 and 200, and, as seen from the results of reference 15 where this effect was measured at $M = 3$ on a 10^o-total-angle cone with various amounts of spherical blunting, no significant change from the perfectly sharp case can be expected until the tip radius Reynolds number is of the order of 7500 or more.

3.3.2 Effect of cooling

At each Mach number the cooling tests were made at constant stagnation pressures of 3, 4 and 5 atmospheres respectively. This range of stagnation pressures was taken so that movement of transition due to cooling could be studied at various positions on the cone. The results are given in Table 1 and are plotted in Figs.5, 6, 7, 8, 11.

The cone was not disturbed between tests at each stagnation pressure, which were made for a range of fixed cooling conditions with the coolant flowing from the base to the tip of the cone and for zero heat transfer with no coolant flowing. Due to surface conduction this latter test with zero coolant flow was not strictly for zero heat transfer (although in the previous section the zero coolant flow condition was given this title, since for this condition zero heat transfer existed on some parts of the cone), and so a datum transition Reynolds number for zero heat transfer for each set was taken from the R_T versus $\frac{T_w}{T_{wo}}$ plots (Figs.5 and 7) for $\frac{T_w}{T_{wo}} = 1$, where T_{wo} for the ratio plotted was calculated assuming a laminar temperature recovery factor of 0.855.

The variation in these datum values for various pressures is probably due to surface condition and pressure gradients along the cone as illustrated in section 3.3.1.

(a) $M_\infty = 3.13$, ($M_1 = 2.93$) and $p_o = 3, 4, 5$ atmospheres

These results are plotted in Figs.5 and 6, and are tabulated in Table 1(1) for the top and bottom generators of the cone. The plots are of the transition Reynolds number based on local flow conditions ($M_1 = 2.93$) against the ratio of a representative surface temperature (T_w, defined in section 3.2), to an estimated surface temperature for zero heat transfer with a laminar boundary layer (T_{wo}), for which, as mentioned earlier, a recovery factor of 0.855 has been assumed.

As discussed in section 3.2 the value for T_w was chosen to be representative of the condition of the laminar boundary layer. Fig.5 shows R_T versus $\frac{T_w}{T_{wo}}$ for the three values of stagnation pressure taken. At 3 and 4 atmospheres stagnation pressure the results for the top and bottom generators of the cone are in close enough agreement for a single mean curve to be drawn through them. However at 5 atmospheres there is a large difference between results on the top and bottom of the cone. This variation is probably due to the cone in this instance being at a slight positive incidence to the airstream, for, although the cone setting in the tunnel was not altered between the sets of tests at each stagnation pressure, the nozzle in the tunnel is two dimensional and profiled on one side only and so it is quite probable that the airstream delivery angle in the working section was changed slightly as stagnation pressure was increased. It must also be remembered that since R_T is directly proportional to the product of stagnation pressure and the distance of transition from the tip, x_T, any errors in measuring the value of x_T would have been far more serious at 5 atmospheres than at 3 atmospheres stagnation pressure. Hence in general more scatter in the results at 5 atmospheres is expected than at 3 or 4 atmospheres.

To eliminate the effect of the variation of transition Reynolds number for zero heat transfer conditions (R_{To}), the results are replotted in Fig.6 as $\frac{R_T}{R_{To}}$ versus $\frac{T_w}{T_{wo}}$, taking the datum R_{To} values from Fig.5 as described earlier in this section. Some collapse is noticed immediately of the 5 atmosphere results, which can now be represented by a single curve.

The Mach number plots in Fig.2 have shown that all the results might have been influenced by the presence of pressure gradients. In particular the variation of transition Reynolds number with stagnation pressure shown in Fig.4(a) for the bottom generator is most likely to have been due to their effect. This suggests for the cooling results an alternative analysis in which more importance is attached to the actual position of transition in the flow field, and in which the transition Reynolds number is assumed to be independent of the stagnation pressure and is a function not only of $\frac{T_w}{T_{wo}}$ but also of the distance x_T along the cone. Hence in the previous analysis for Fig.6 a transition Reynolds number obtained with cooling should have been compared with the transition Reynolds number for zero heat transfer measured at the same transition position, although the latter case would have corresponded in practice to a different stagnation pressure.

In order to illustrate this method Fig.9 has been constructed. The lower graph in this figure shows the variation of R_{To} with distance from the cone

tip, x_T, for all the zero heat transfer results at $M = 3$ on the bottom generator of the cone, and is an alternative plot to the one in Fig.4(a). The upper graph shows R_T versus x_T obtained with cooling on the bottom generator at 4 atmospheres stagnation pressure, and the appropriate datum R_{T_o} value from Fig.5(b) has been inserted on the mean line through these results. A line parallel to that of the R_{T_o} versus x_T plot has then been constructed through this datum point, as illustrated, and the assumption has been made that this gives the correct variation of the datum zero heat transfer transition Reynolds number with x_T on the bottom generator. Fig.10(a) was then produced by taking the ratio of the transition Reynolds number for each cooling condition $\frac{T_w}{T_{wo}}$ to the estimated datum value of the zero heat transfer Reynolds number which occurred at the same x_T value in Fig.9.

Comparison in Fig.10(a) of these results with their former values from Fig.6(b) shows that the net effect of this new analysis is to steepen the mean curve through the results, although a similar analysis on the top generator for the same stagnation pressure produced little change, for as mentioned earlier (section 3.3.1) R_{T_o} on this generator was practically constant for all values of stagnation pressure (and hence x_T). The same trend was true also for the results at the other stagnation pressures and Fig.10(b) shows this effect on the complete band of results. It is to be hoped that this method of analysis will have lessened any pressure gradient effect which might have been present.

(b) $M_\infty = 3.8$, $(M_1 = 3.48)$ and $p_o = 3, 4, 5$ atmospheres

These results are plotted in Figs.7, 8 and are tabulated in Table 1(2) for the top and bottom generators of the cone. The plotting details of Figs. 7, 8 are exactly those of Figs.5, 6, respectively.

In Fig.7 the disagreement of the results on the top and bottom generators is again almost certainly due to the cone being finally set at a slight positive incidence to the airstream.

The datum zero heat transfer Reynolds numbers for the ratio $\frac{R_T}{R_{T_o}}$ for Fig.8 were taken from Fig.7.

As before, plots similar to those in Fig.3 indicated quite clearly at this Mach number that all these results might have been subjected to pressure gradients, and so the alternative analysis of the results was made. The result of this analysis was to steepen the mean curves through the results in Fig.8 for both generators and the order of this effect can be seen in Fig.10(c) which was constructed in the same way as Fig.10(b).

(c) Comparison of cooling results and effect of Mach number on cooling

In Fig.11 bands of results of $\frac{R_T}{R_{T_o}}$ versus $\frac{T_w}{T_{wo}}$ for both $M = 3$ and $M = 4$ have been plotted. These bands represent the sum of the bands obtained earlier by alternative analyses for each Mach number and were taken from Figs.10(b) and 10(c) respectively.

Curves derived from results contained in references 13 and 14 for a $9\frac{1}{2}^{\circ}$ sharp cone in a $M_{\infty} = 3.12$ airstream (giving $M_1 = 3.0$) are shown for comparison with the above M = 3 results. The models used in these tests were all $9\frac{1}{2}^{\circ}$ cone-cylinders with different amounts of blunting, but in deriving the mean curves shown only the results with transition actually occurring on the cone portion for the sharpest tip were used.

In fact the mean curve obtained from Ref.13 is also representative of the mean curve of results obtained at M = 3 in the Bedford test[6] for the 15° cone. The results for the $M_1 = 1.86$ tests at Bedford have also been included in Fig.11.

Although the results of the present tests fall into such wide bands they are sufficiently good to show quite clearly that the cooling effectiveness, found to decrease in the Bedford tests[6] on increasing local Mach number (M_1) for 1.86 to 2.81, continues to decrease when M_1 is further increased to 3.48.

As an example of the order of this decrease of cooling effectiveness with increasing Mach number, it follows from Fig.11 that at a local Mach number (M_1) of 2.93 when the surface temperature ratio T_w/T_{wo} is reduced from 1.0 to 0.85 the transition Reynolds number at zero incidence is increased by a factor of about 1.3 - 1.45, whereas the same reduction in surface temperature ratio at a local Mach number of 3.48 produces only an increase of about 1.1 - 1.25.

4 RESULTS AND DISCUSSION OF TESTS AT AN INCIDENCE OF $+2^{\circ}$

For these tests the 15° steel cone was set at an incidence of $+2^{\circ}$ and was again cooled from the base to the tip.

Earlier work at $+2^{\circ}$ on a 15° steel cone had been done for the zero heat transfer case[7] at nominal free stream Mach numbers of 3 and 4, and the cooled case[6] at nominal free stream Mach numbers of 2 and 3. These tests had found that a marked difference in transition position between the top (leeward) and the bottom (windward) generator exists at incidence, and the indications were that little or no movement of transition position on the leeward generator could be induced by cooling, although transition on the windward generator behaved as at zero incidence.

Since changes in local Mach number and Reynolds number caused by varying the incidence of the 15° cone from 0° to $+2^{\circ}$ are slight, the analysis of the present test results is based on values of these derived from zero incidence. By this means a direct comparison of the incidence results with those of section 3 is obtained, and the effect of an error is an intended zero incidence setting for a flight case is clearly shown.

For these tests also the condition of theoretical zero pressure gradient is still valid along the generators of the cone except near the tip.

4.1 Surface temperature distributions

Surface temperature distributions on the top and bottom generators of the 15° steel cone for various amounts of wall cooling at $+2^{\circ}$ incidence for $M_{\infty} = 3.13$ and $p_o = 5$ atmospheres are given in Fig.12. The solid curves in the figure refer to the top (leeward) generator and the broken curves to the bottom (windward) generator. Transition positions, which were found from shadowgraph pictures, are indicated by short vertical lines through these curves.

The distributions shown in Fig.12 are typical also of most of the results obtained at p_o = 3 and 4 for the same incidence and Mach number. However, due to the low Reynolds number per inch per atmosphere stagnation pressure at this Mach number, transition disappeared with cooling off the end of the cone on the bottom (windward) generator for the latter stagnation pressures. For these cases the temperature distribution on the bottom generator remained entirely below that on the top generator for the whole length of the cone, although the difference between these distributions was never more than 3°C.

At M_∞ = 3.8 transition did not occur at all on the bottom generator at stagnation pressures of 3, 4 and 5 atmospheres, for the Reynolds number per inch per atmosphere was too small at this Mach number. As a result all the temperature distributions were of the latter kind above.

Due to the lack of thermocouple stations no measurement of temperature was made nearer the tip of the cone than 2.6 inches. Hence, since transition positions on the top and bottom generators are so widely apart in these tests, the station situated at 2.6 inches from the tip on the top generator was chosen as the representative temperature in the laminar region for both generators. (This is a fairly arbitrary choice and here again an error of 3°C would correspond to 0.01 in $\frac{T_w}{T_{wo}}$ in Figs.13, 14).

4.2 Results from shadowgraph pictures

The results obtained from shadowgraph pictures are tabulated in Tables 2(1) and 2(2) and are shown in Figs.13 and 14, as plots of transition Reynolds number (based on local flow conditions appropriate to the zero incidence case) against the ratio $\frac{T_w}{T_{wo}}$, where T_{wo} is the zero heat transfer temperature for a laminar boundary layer, assuming a recovery factor of 0.855 and zero incidence flow conditions.

Fig.13 is for M_∞ = 3.13 and shows at once the marked difference which exists between results on the top (leeward) and bottom (windward) generators. The curves of Fig.5 are added to this figure to illustrate the fact that the transition Reynolds number on the windward side varied with $\frac{T_w}{T_{wo}}$ at about the same rate as at zero incidence, as was shown in the Bedford tests[6] at nominal M = 2 and M = 3. On the leeward side, however, little or no effect on the transition Reynolds number was obtained either by cooling (also found in the Bedford tests), or by change of stagnation pressure, for transition always occurred at about $\frac{3}{4}$ of an inch to an inch back from the tip of the cone irrespective of the values of p_o or $\frac{T_w}{T_{wo}}$.

Fig.14 is for M_∞ = 3.8 and, as mentioned earlier, transition did not occur at all on the windward generator. On the top generator it was found again that the transition position was more or less invariant at about $1\frac{3}{4}$ to $2\frac{1}{4}$ inches from the tip and was hardly affected at all by cooling or change of stagnation pressure.

The probable cause of this immobility of the transition position on the top generator with cooling for both these Mach numbers is that the cross-flows introduced by setting the cone at incidence dominate the flow on this leeward side to such an extent that transition is triggered off regardless of the surface temperature.

5 CONCLUSIONS

Measurements of boundary layer transition (from shadowgraph pictures) on a 15° cone in a wind tunnel at M_∞ = 3.13 and 3.8 gave the following results.

5.1 With the cone set at zero incidence to the airstream.

(1) For zero heat transfer conditions at M_∞ = 3.13 the transition Reynolds number was approximately constant on the top generator at about 2.9 million for a range of stagnation pressures from 2 to 5 atmospheres (Fig.4(a)), but on the bottom generator it varied linearly from about 2.5 million at 2 atmospheres to 3.1 million at 5 atmospheres stagnation pressure. The pressure gradients present on the cone may have had some influence in the latter case.

(2) At M_∞ = 3.8, the zero heat transfer Reynolds number increased roughly from 2.4 million on the top generator and 2.5 million on the bottom generator at 3 atmospheres stagnation pressure, to 3.0 million on the top and 3.1 million on the bottom generator at 5 atmospheres stagnation pressure (Fig.4(b)). The variation of approximately 0.1 million between the results on the two generators at each stagnation pressure is almost certainly due to the cone being at a slight positive incidence to the airstream. Whereas the increase in transition Reynolds number with stagnation pressure may again be due to the pressure gradients present.

(3) The variation of transition Reynolds number with surface temperature ratio $\frac{T_w}{T_{wo}}$ was far less at M_∞ = 3.8 than at M_∞ = 3.13. Alternative analyses of the test results, which were made because of the dependence of transition Reynolds number for zero heat transfer conditions on stagnation pressure, showed that for the reduction in $\frac{T_w}{T_{wo}}$ from 1.0 to 0.85 R_T would be increased by a factor of about 1.3 - 1.45 at a local Mach number (M_1) of 2.93 and by a factor 1.1 - 1.25 for M_1 = 3.48 (Fig.11).

5.2 With the cone set at 2 degrees positive incidence.

(1) At M_∞ = 3.13, the transition Reynolds number on the bottom (windward) generator varied with the ratio $\frac{T_w}{T_{wo}}$ at about the same rate as was found in the zero incidence tests (Fig.13). However on the top (leeward) generator little or no movement of the transition point occurred when the cone was cooled.

(2) At M_∞ = 3.8 transition did not occur on the cone on the windward generator and only results from the leeward generator were obtained (Fig.14). Here again little or no movement of the transition point occurred when the cone was cooled, and it appears that at both Mach numbers the cross-flows introduced on setting the cone at incidence dominate the flow character on this leeward side.

LIST OF SYMBOLS

M	Mach number
M_∞	Mach number in working section of tunnel, ahead of tip shock wave of cone
M_1	local Mach number outside boundary layer on cone surface
p_o	stagnation pressure absolute (atmospheres)
r	temperature recovery factor $= \dfrac{T_{wo} - T_1}{T_{H_1} - T_1}$, where T_1 is static temperature of stream outside boundary layer, T_{wo} and T_{H_1} are defined below
R_T	transition Reynolds number based on local flow conditions $= \dfrac{u_1 x_T}{\nu_1}$, where u_1 and ν_1 are the velocity and kinematic viscosity of the stream outside the boundary layer, and x_T is defined below
R_{To}	transition Reynolds number under zero heat transfer conditions, again based on local conditions $= \dfrac{u_1 x_{To}}{\nu_1}$, where x_{To} is defined below
T_{H_1}	stagnation temperature, equal to total temperature outside boundary layer (^oK or ^oC)
T_w	temperature of cone surface (^oK or ^oC)
T_{wo}	value of T_w under zero heat transfer conditions (^oK or ^oC)
x	distance from tip along generator of cone (inches)
x_T	value of x at the transition point from laminar to turbulent flow (inches)
x_{To}	value of x_T under zero heat transfer conditions

LIST OF REFERENCES

No.	Author	Title, etc.
1	Lees, L.	The stability of the laminar boundary layer in a compressible fluid. NACA Report 876, 1947. NACA TN 1360.
2	Van Driest, E.R.	Calculation of the stability of the laminar boundary layer in a compressible fluid on a flat plate with heat transfer. Journal of the Aeronautical Sciences Vol.19, p.801, December 1952.
3	Dunn, D.W. Lin, C.C.	On the stability of the laminar boundary layer in a compressible fluid. Journal of the Aeronautical Sciences Vol.22, p.455, July 1955.
4	Morduchow, M. Grape, R.G.	Separation, stability and other properties of compressible laminar boundary layer with pressure gradient and heat transfer. NACA Tech. Note No. 3296, May 1955.
5	Monaghan, R.J.	A survey and correlation of data on heat transfer by forced convection at supersonic speeds. ARC R & M 3033. September 1953
6	Browning, A.C. Crane, J.F.W. Mon ghan, R.J.	Measurements of the effect of surface cooling on boundary layer transition on a 15° cone. Part 1. Tests at M = 2 and 3 in an 8 in. x 9 in. wind tunnel at RAE Bedford. CP 381. September 1957.
7	Davies, F.V. Monaghan, R.J.	Boundary layer measurements on 15° and 24.5° cones at small angles of incidence at M = 3.17 and 3.82 and zero heat transfer. R & M 3133. 1957.
8	Crane, J.F.W. Browning, A.C.	A comparison between several methods of detecting boundary layer transition in high speed flow. RAE Tech. Note Aero (to be issued).
9	Crane, J.F.W.	The use of woollen felt screens as air cleaners in supersonic wind tunnels. RAE Tech. Note Aero (to be issued).
10	Crane, J.F.W.	The effect of humidity on laminar recovery temperature measurements in supersonic flow of air in wind tunnels. Unpublished M.O.S. Report.
11	Buchele, D.R. Goossens, H.R.	Lens system producing unequal magnification in two mutually perpendicular directions. Review of scientific instruments Vol.25, No.3, p.262, March 1954.

LIST OF REFERENCES (Contd)

No.	Author	Title, etc.
12	Midwood, G.F. Hayward, R.W.	An automatic self-balancing capsule manometer. CP 231. July 1955
12	Jack, J.R. Diaconis, N.S.	Variation of boundary-layer transition with heat transfer on two bodies of revolution at a Mach number of 3.12. NACA TN 3562, September 1955.
14	Diaconis, N.S. Jack, J.R. Wisniewski, R.J.	Boundary layer transition at Mach 3.12 as affected by cooling and nose blunting. NACA TN 3928, January 1957.
15	Brinich, P.F. Sands, N.	Effect of bluntness on transition for a cone and a hollow cylinder at Mach 3.1. NACA TN 3979, May 1959.

APPENDIX 1

DETAILS OF THE SETTLING CHAMBER, FILTERS, TURBULENCE LEVEL AND HUMIDITY

The settling chamber consisted of two 21 inch lengths of 18 inch bore steel pipe, which were situated just upstream of the working section (Figs. 1(a) and 1(b)).

Upstream of the settling chamber was a 12 inch length of the same pipe and this contained 4 felt filters. These filters[9] served a dual purpose by both removing dust from the airstream and reducing the turbulence level within it. An indication of the turbulence reduction in the airstream produced by introducing filters to this section of pipe was obtained by observing the gain in the transition Reynolds number on the cone for zero heat transfer and fixed stagnation pressure and temperature, and it was found that only the addition of the first filter produced a significant increase. This suggests that the turbulence level in the airstream was low after damping by this filter, although the final level present in the stagnation chamber was probably fixed by a 2" mesh stagnation temperature measuring grid (section 2.3.3) which was fitted just downstream of the filters.

A dew-point meter, sampling at the high pressure end of the tunnel, was used to check the humidity of the air supplied to the system from the compressors. Careful check was made on the humidity level throughout each test, and all the results contained in this note are for a value of absolute humidity less than 4.5×10^{-4} lb/lb, which would have the effect, according to Ref.10, of increasing zero heat transfer temperature on the model for both Mach numbers by less than 1.2°C above that obtained with perfectly dry air. This low level of humidity also ensured the absence of strong condensation shocks in the nozzle region[10], which could have altered appreciably the flow direction in the working section, since the nozzle was single-sided, and hence given the model an effectively unknown change of incidence.

TABLE 1

Test results showing the effect of surface cooling on transition position at zero incidence (as determined by shadowgraph)

(1) $M_\infty = 3.13$, $(M_1 = 2.93)$. $\frac{T_{wo}}{T_{H_1}}$ assumed to be 0.908 (corresponding to a laminar recovery factor of 0.855). The coolant flowing from the base to the tip of the cone. $T_{H_1} \simeq 35°C$. T_w is a representative laminar boundary layer temperature (section 3.2).

(a) $p_o = 3$ atm.

Test	T_{wo} °K	$\frac{T_w}{T_{wo}}$	R_T millions	
			Top generator	Bottom generator
A	280.1	1.001	2.92	2.78
	280.4	0.840	3.80	3.67
	280.8	0.883	3.42	3.34
	280.4	0.938	2.98	-

From Fig.5(a) R_{T_o} (top and bottom) is taken to be 2.85 when evaluating $\frac{R_T}{R_{T_o}}$ in Fig.6(a).

(b) $p_o = 4$ atm.

B	278.4	1.004	2.92	2.89
	279.7	0.863	4.15	3.94
	279.4	0.922	3.43	3.43
	280.5	0.955	3.07	3.14
C	280.7	1.004	2.89	2.96
	279.9	0.923	3.46	3.29
	279.5	0.959	3.07	3.14

From Fig.5(b) R_{T_o} (top and bottom) is taken to be 2.92 when evaluating $\frac{R_T}{R_{T_o}}$ in Fig.6(b).

(c) $p_o = 5$ atm.

D	280.7	1.008	2.91	3.09
	275.7	0.874	3.93	4.20
	279.9	0.908	3.65	4.03
	280.2	0.971	3.12	3.56

From Fig.5(c) R_{T_o} (top) and R_{T_o} (bottom) are taken to be respectively 2.95 and 3.22 when evaluating $\frac{R_T}{R_{T_o}}$ in Fig.6(c).

(2) $M_\infty = 3.8$, ($M_1 = 3.48$). $\frac{T_{wo}}{T_{H_1}}$ assumed to be 0.897 (corresponding to a laminar recovery factor of 0.855). The coolant flowing from the base to the tip of the cone. $T_{H_1} \simeq 40^\circ C$. T_w is a representative laminar boundary layer temperature (section 3.2).

(a) $p_o = 3$ atm.

Test	T_{wo} °K	$\frac{T_w}{T_{wo}}$	R_T millions	
			Top generator	Bottom generator
E	283.5	1.018	2.3	2.56
	280.7	0.884	2.68	2.78
	282.0	0.858	2.71	2.82
	282.4	0.850	2.73	2.88
	282.3	0.889	2.65	2.73
	282.1	0.909	2.61	2.7
	281.8	0.946	2.4	2.67
F	285.7	0.886	2.57	2.78
	286.0	0.902	2.57	2.71
	284.0	1.02	2.45	2.56

From Fig.7(a) R_{T_o} (top) and R_{T_o} (bottom) are taken to be respectively 2.37 and 2.58 when evaluating $\frac{R_T}{R_{T_o}}$ in Fig.8(a).

(b) $p_o = 4$ atm.

G	284.8	1.010	2.73	2.85
	284.0	0.852	3.06	3.23
	284.3	0.876	3.00	3.29
	283.4	0.916	2.90	3.09
	282.5	0.949	2.87	3.10
	283.4	0.967	2.83	2.99

From Fig.7(b) R_{T_o} (top) and R_{T_o} (bottom) are taken to be respectively 2.75 and 2.86 when evaluating $\frac{R_T}{R_{T_o}}$ in Fig.8(b).

(c) $p_o = 5$ atm.

H	281.3	1.012	3.0	3.21
	283.1	0.966	3.15	3.29
	283.7	0.943	3.16	3.28
	284.3	0.890	3.33	3.42
	284.8	0.867	3.36	3.49
	284.4	0.855	3.41	3.71

From Fig.7(c) R_{T_o} (top) and R_{T_o} (bottom) are taken to be respectively 3.03 and 3.22 when evaluating $\frac{R_T}{R_{T_o}}$ in Fig.8(c).

TABLE 2

Test results showing the effect of surface cooling on transition position at +2° incidence (as determined by shadowgraph)

(1) $M_\infty = 3.13$. $\frac{T_{wo}}{T_{H_1}}$ assumed to be 0.908 (corresponding to a laminar boundary layer with recovery factor 0.855 and zero incidence flow conditions $M_1 = 2.93$). The coolant flowing from the base to the tip of the cone. $T_{H_1} \simeq 35^\circ C$. T_w is the surface temperature at the point on the top generator 2.6 inches from the tip.

(a) $p_o = 3$ atm.

Test	T_{wo} °K	$\frac{T_w}{T_{wo}}$	R_T millions	
			Top generator	Bottom generator
I	277.2	1.013	0.55	3.56
	276.7	1.013	0.60	> 3.83
	275.7	0.896	0.41	> 3.86
	278.2	0.949	0.41	> 3.79

(b) $p_o = 4$ atm.

J	277.2	1.014	-	3.82
	278.7	0.888	-	> 4.74
	275.0	0.927	0.71	4.50
	273.6	0.974	0.71	4.36
	273.1	1.018	0.71	4.01

(c) $p_o = 5$ atm.

K	277.8	1.016	0.80	4.35
	274.1	0.906	0.91	5.20
	273.0	0.938	0.91	4.80
	277.6	0.953	0.76	4.93

(2) $M_\infty = 3.8$. $\frac{T_{wo}}{T_{H_1}}$ assumed to be 0.897 (corresponding to a laminar boundary layer with recovery factor 0.855 and zero incidence flow conditions $M_1 = 3.48$). The coolant flowing from the base to the tip of the cone. $T_{H_1} \simeq 35^\circ C$. T_w is the surface temperature at the point on the top generator 2.6 inches from the tip. Transition did not occur on the bottom generator.

(a) $p_o = 3$ atm.

Test	T_{wo} °K	$\frac{T_w}{T_{wo}}$	R_T millions / Top generator
L	281.1	1.011	0.97
	279.1	0.984	0.88
	279.1	0.943	0.88
M	283.2	1.008	0.83

(b) $p_o = 4$ atm.

N	277.7	1.014	0.97
	279.3	0.899	0.97
	279.6	0.939	0.99
	280.4	0.983	0.99
O	281.7	1.012	1.04
	281.8	0.892	1.03
	282.0	0.930	1.02
	282.3	0.969	1.02

(c) $p_o = 5$ atm.

P	281.8	1.014	1.06
	281.3	0.893	1.20
	281.4	0.930	1.06
	281.4	0.972	1.06
	281.3	1.004	1.06

WT.2078.C.P.479.K3 - Printed in England

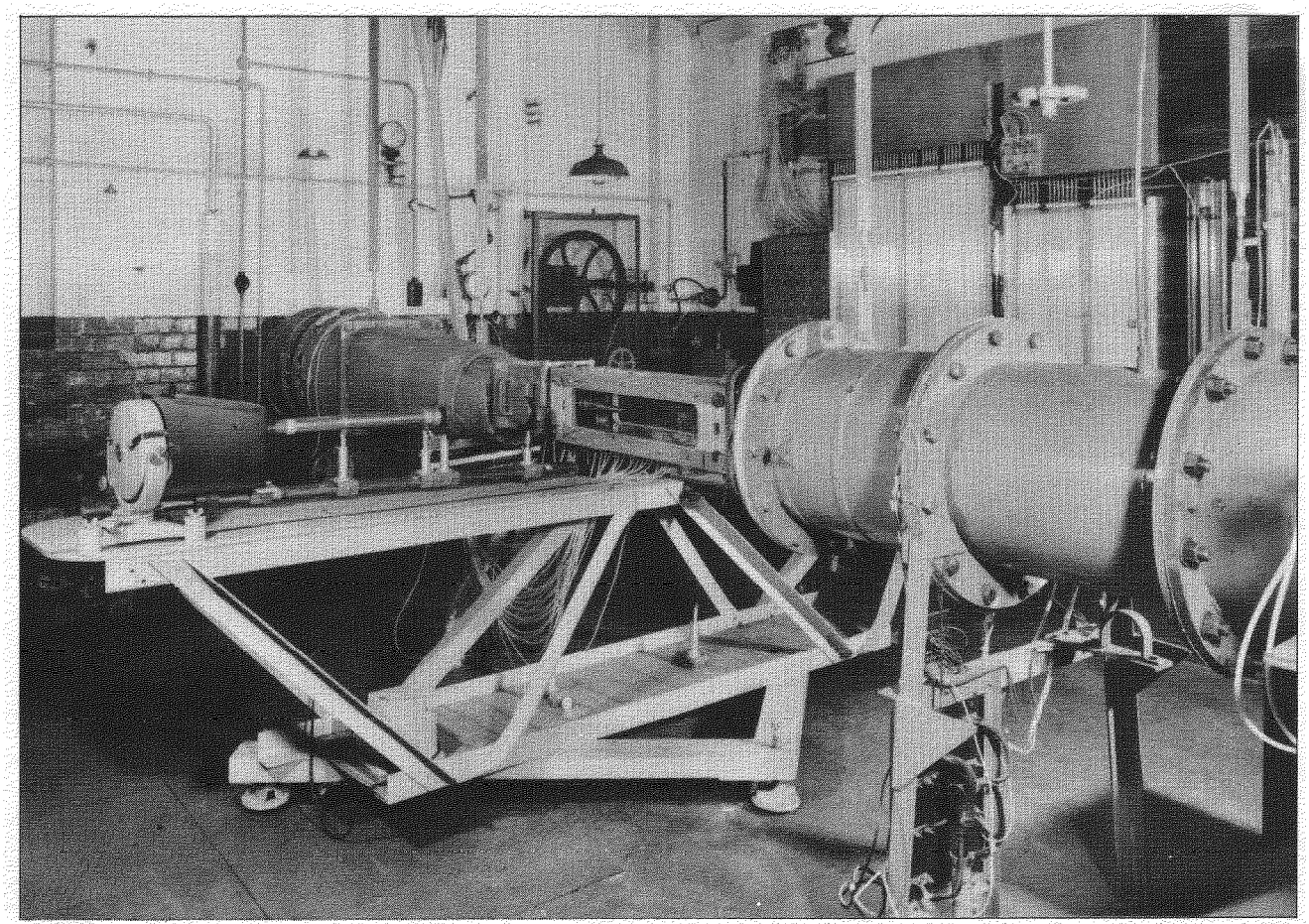

FIG.1a. VIEW TOWARDS DIFFUSER, SHOWING OPTICAL BENCH, MANOMETER BANK AND THE POSITION OF THE CONE IN THE WORKING SECTION

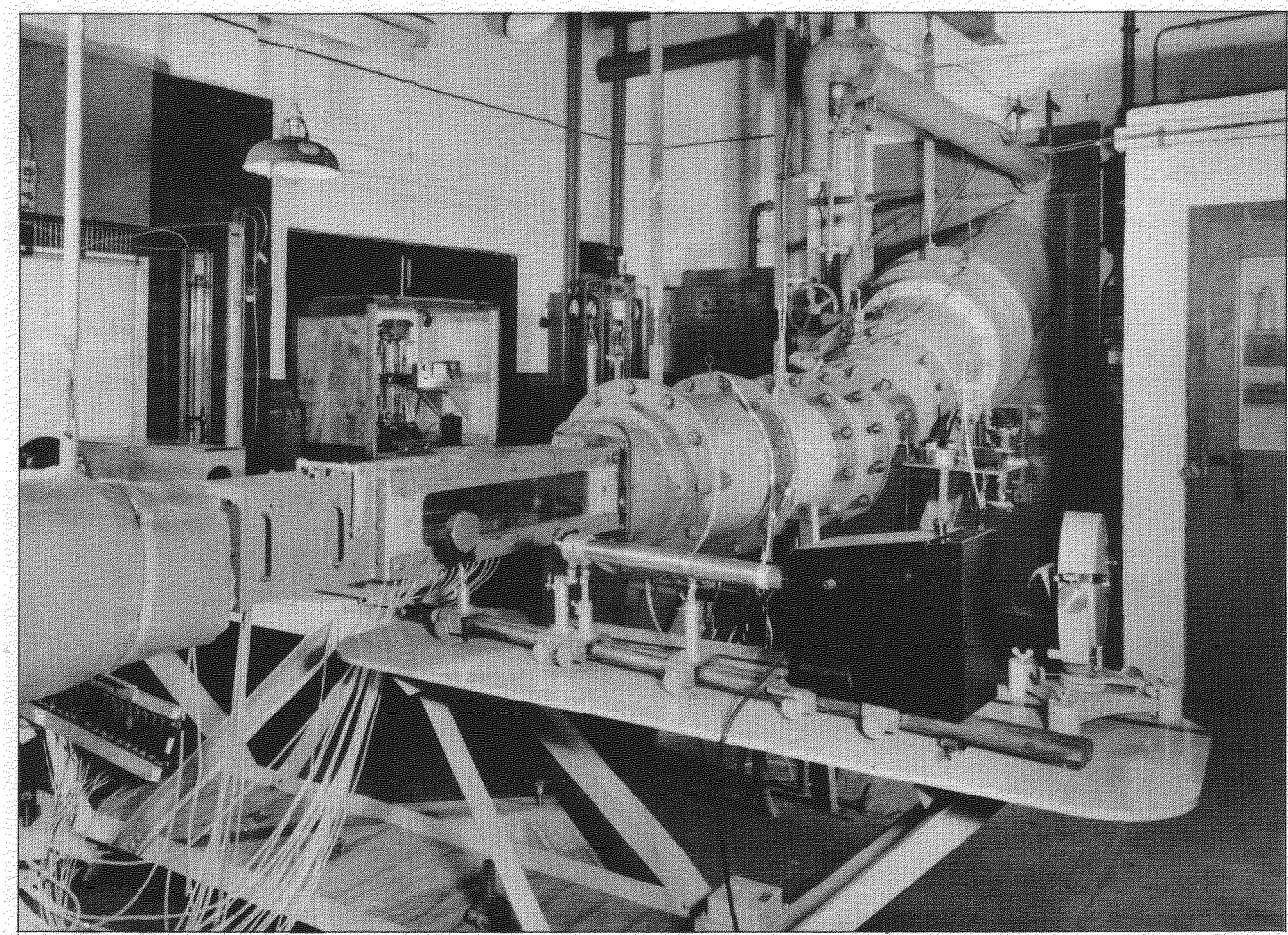

FIG.1b. VIEW TOWARDS SETTLING CHAMBER, SHOWING OPTICAL BENCH AND HYGROMETER

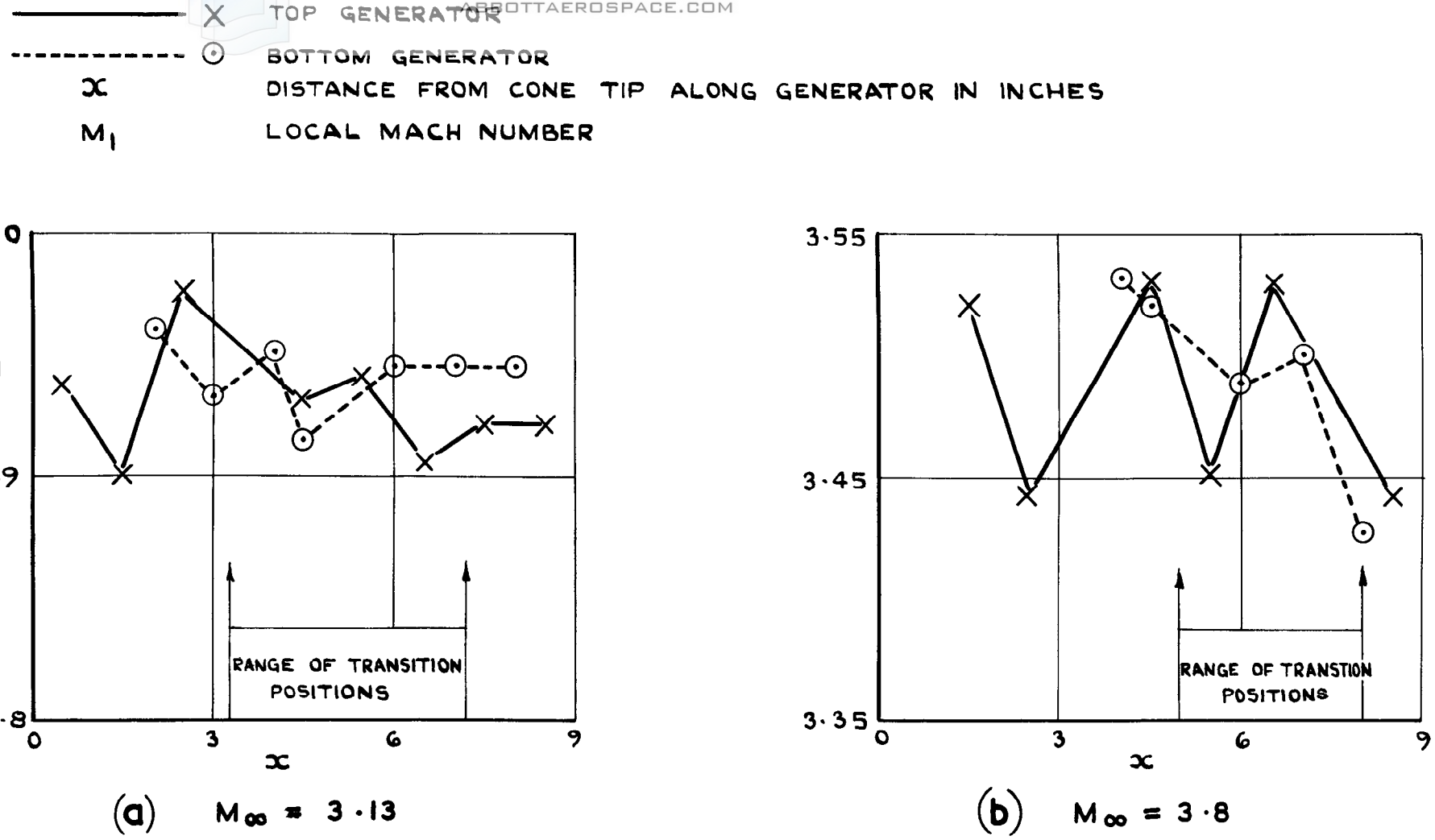

FIG. 2. (a & b) DISTRIBUTIONS OF LOCAL MACH NUMBER ALONG THE 15° COPPER CONE FOR A STAGNATION PRESSURE (P_o) OF 4 ATMOS. (ZERO INCIDENCE.)

(TRANSITION POSITIONS FROM SHADOWGRAPH SHOWN BY VERTICAL LINES ACROSS CURVES. ——X TOP GENERATOR - - - - - - -⊙ BOTTOM GENERATOR)

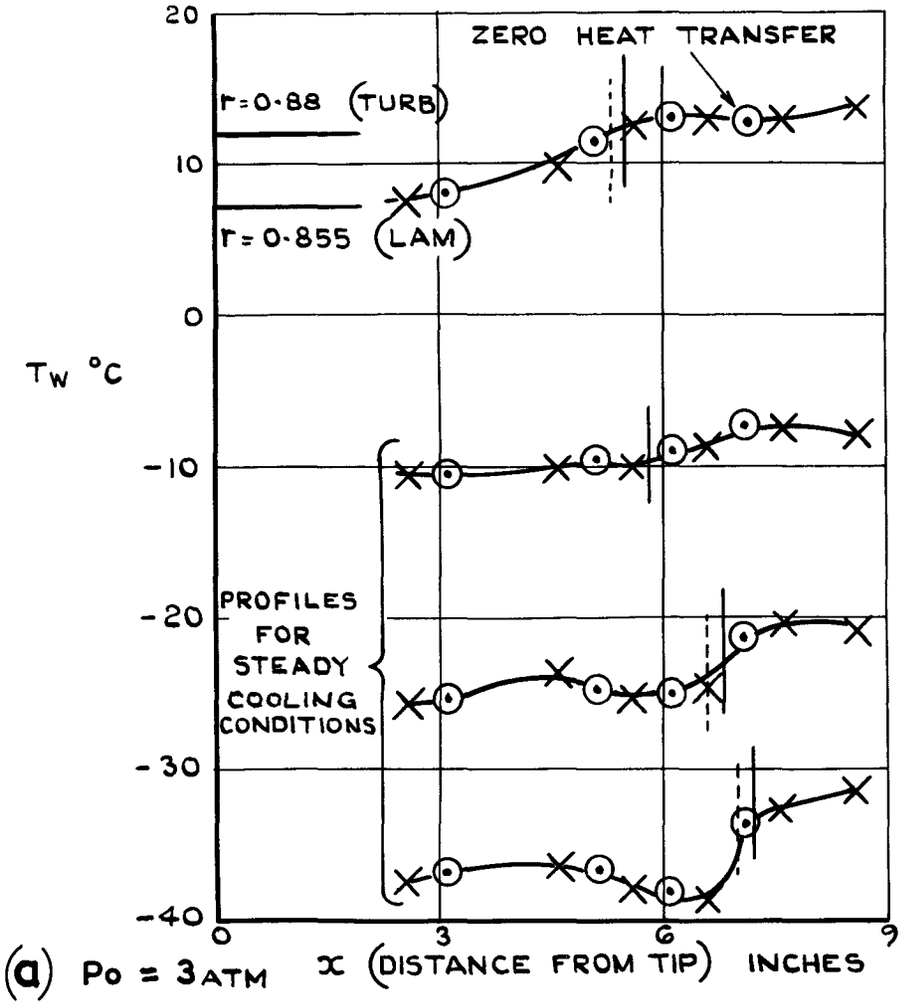

(a) P_o = 3 ATM

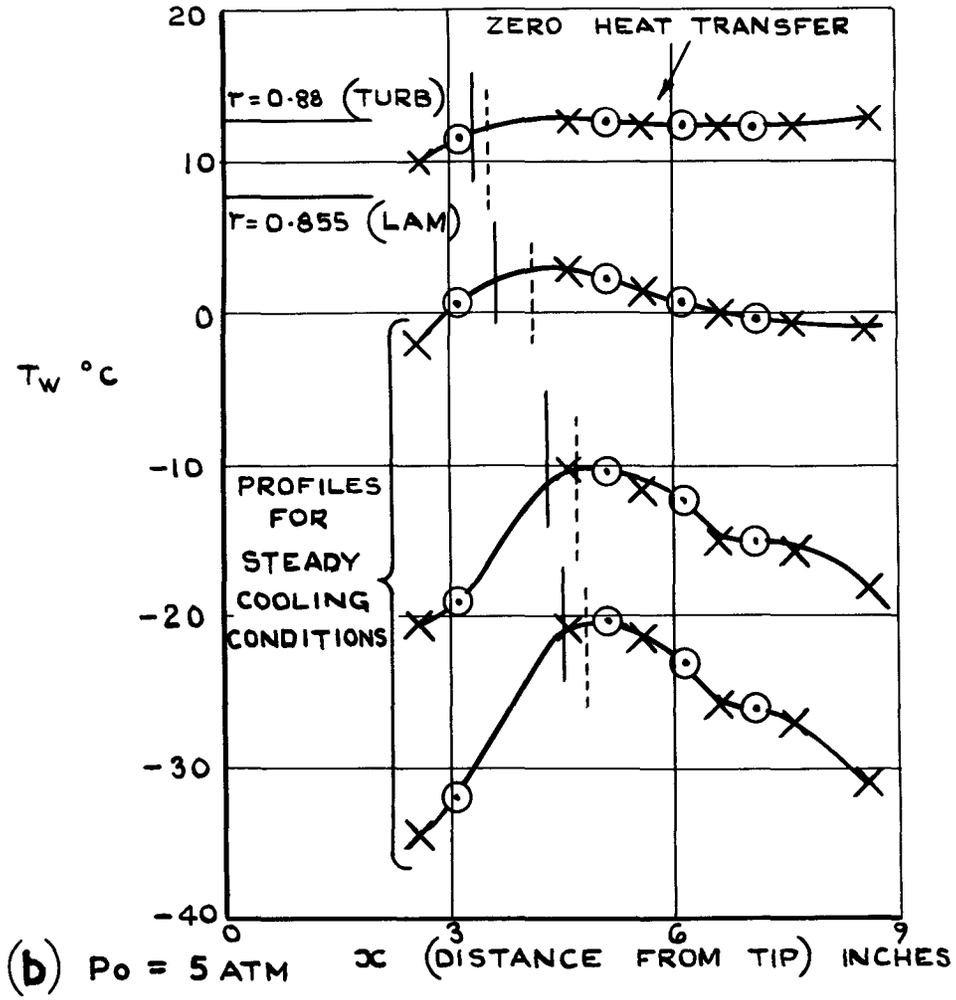

(b) P_o = 5 ATM

FIG. 3. (a & b.) TYPICAL DISTRIBUTIONS OF SURFACE TEMPERATURE ALONG THE 15° STEEL CONE AT $M_\infty = 3{\cdot}13$ WITH COOLANT FLOWING FROM BASE TO TIP (ZERO INCIDENCE.)

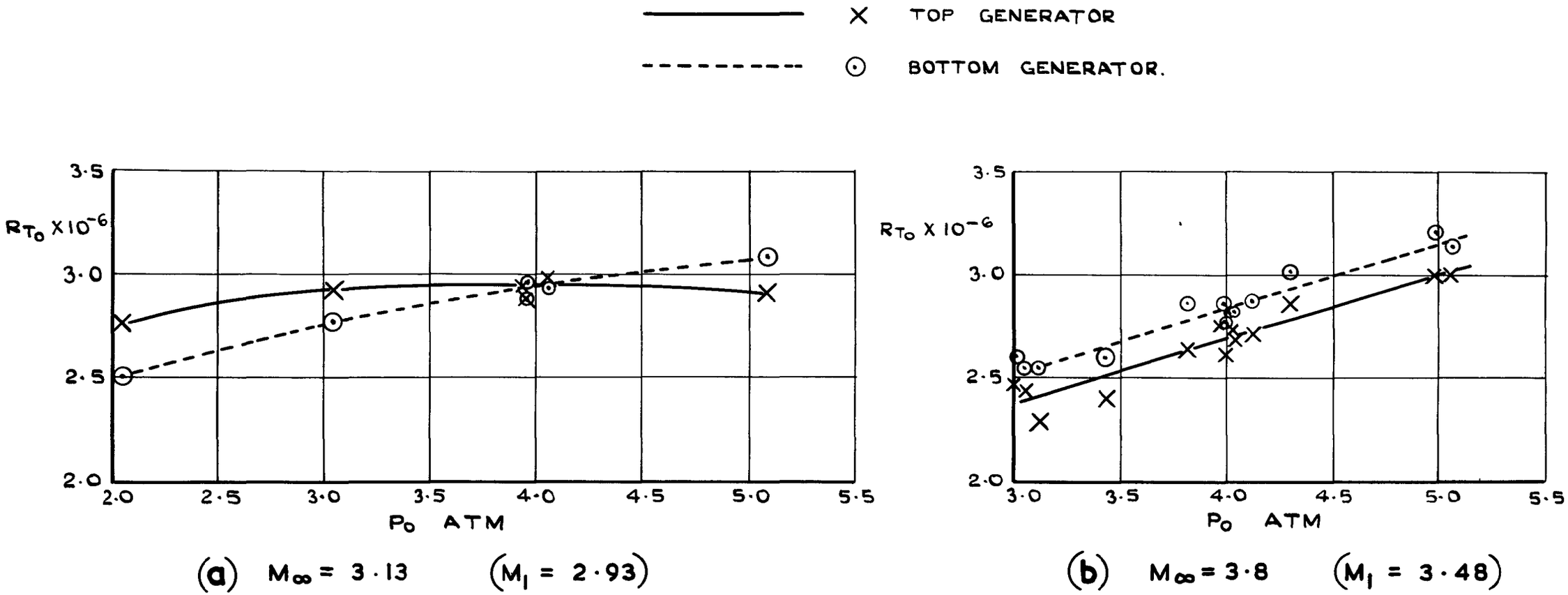

FIG. 4. (a & b) TRANSITION REYNOLDS NUMBERS (FROM SHADOWGRAPH) UNDER ZERO HEAT TRANSFER CONDITIONS. (ZERO INCIDENCE.)

× TOP GENERATOR
⊙ BOTTOM GENERATOR

T_w IS A REPRESENTATIVE LAMINAR WALL TEMP. (SEE SECTION 3·2)

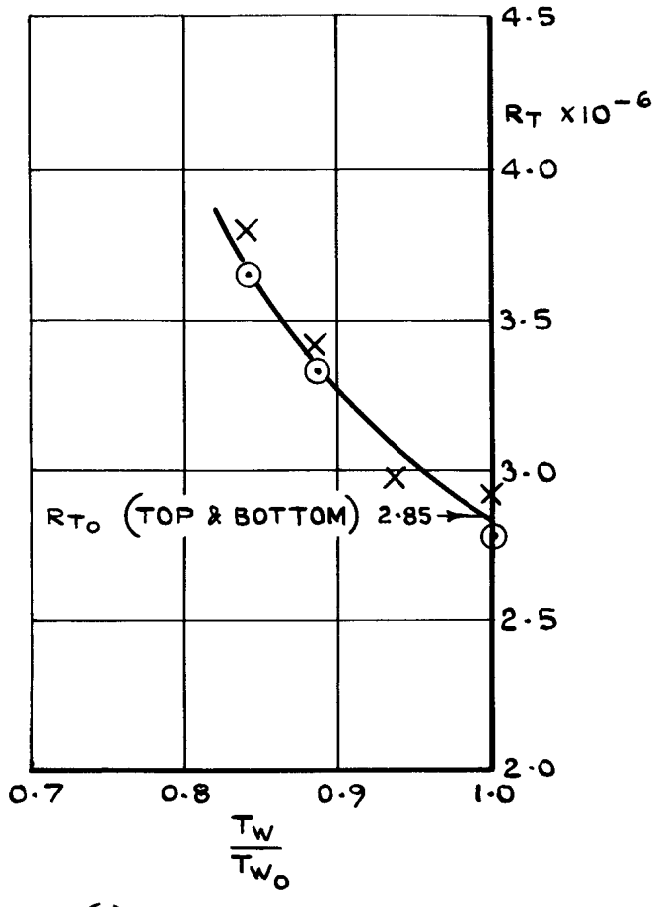

(a) P_o = 3 ATM

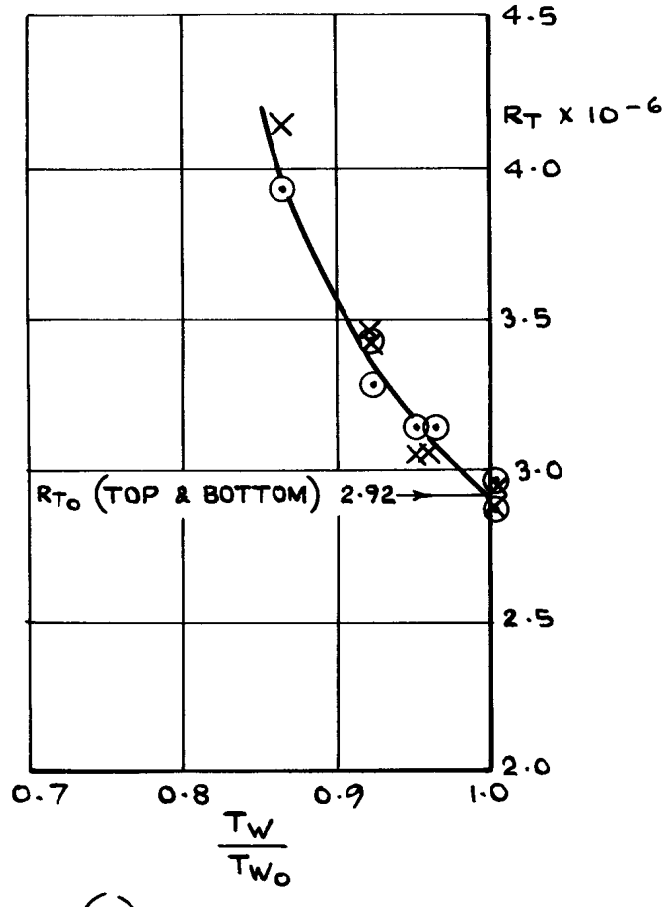

(b) P_o = 4 ATM

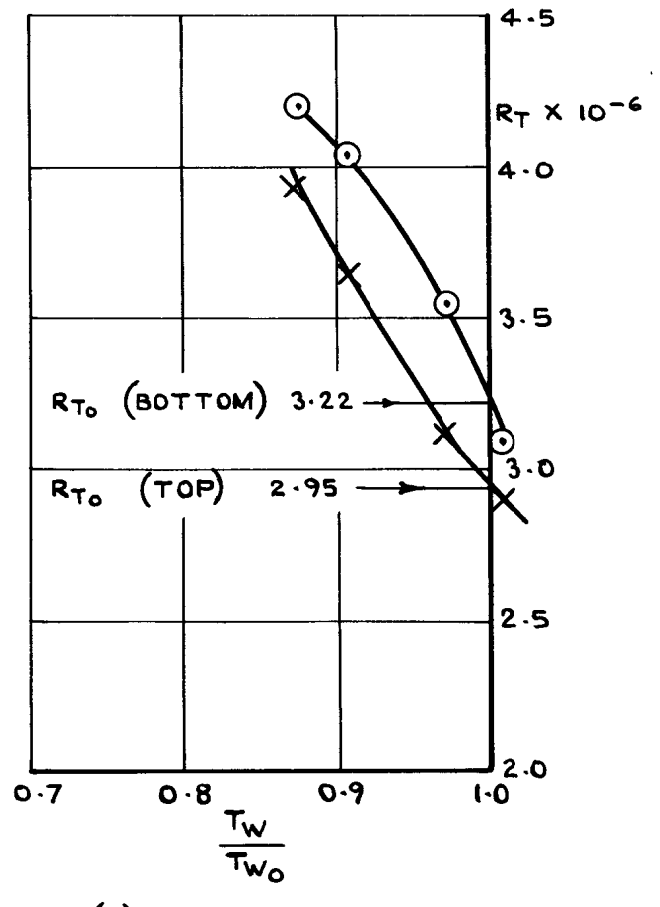

(c) P_o = 5 ATM

FIG. 5. (a b & c) EFFECT OF COOLING ON TRANSITION REYNOLDS NUMBER (FROM SHADOWGRAPH) AT $M_\infty = 3 \cdot 13$ ($M_1 = 2 \cdot 93$) AND $P_o = 3-5$ ATM. (ZERO INCIDENCE.)

× TOP GENERATOR
⊙ BOTTOM GENERATOR.

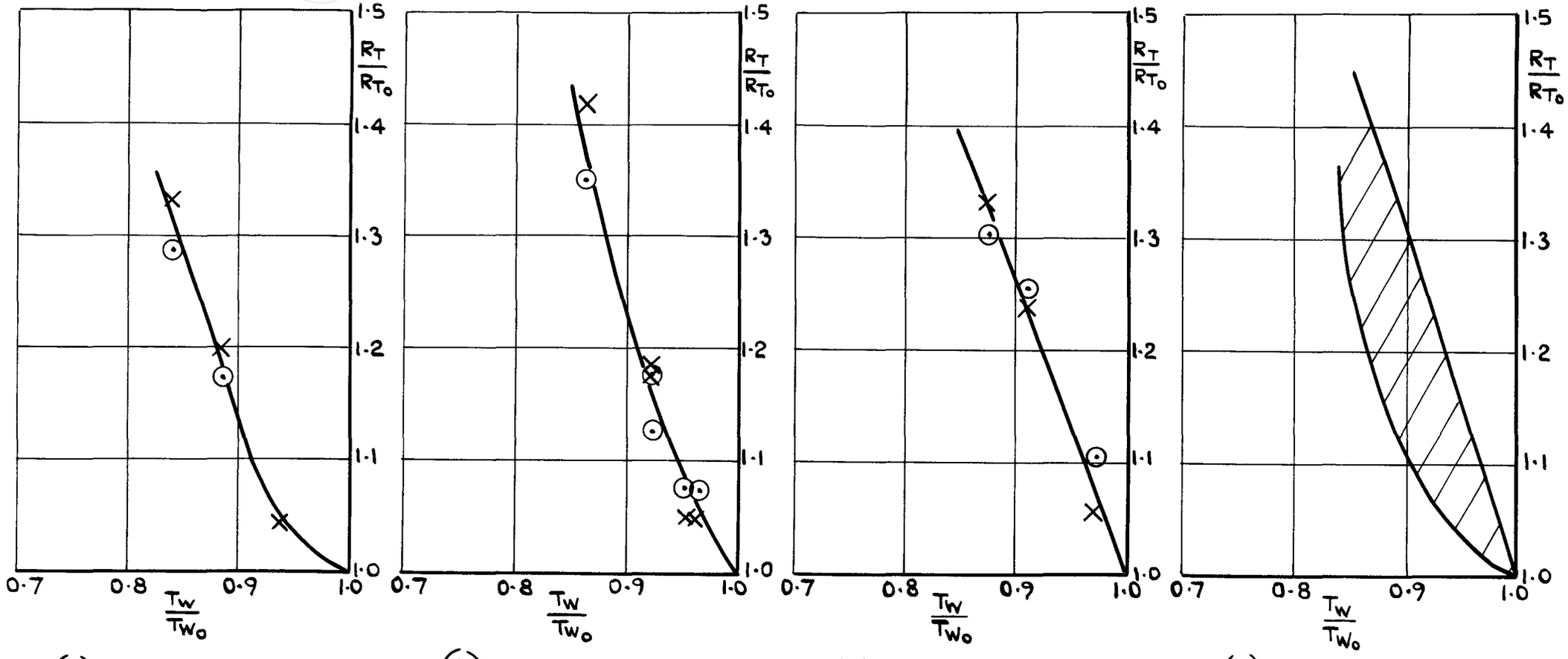

(a) P_o = 3 ATM (b) P_o = 4 ATM (c) P_o = 5 ATM (d) BAND COVERING RESULTS (a), (b), & (c).

FIG. 6. (a, b, c, & d) EFFECT OF COOLING ON TRANSITION REYNOLDS NUMBER (FROM SHADOWGRAPH) AT $M_\infty = 3{\cdot}13$, ($M_1 = 2{\cdot}93$), AND $P_o = 3-5$ ATM. (ZERO INCIDENCE)
(R_{T_o} VALUES USED BEING THOSE INDICATED IN FIG. 5.)

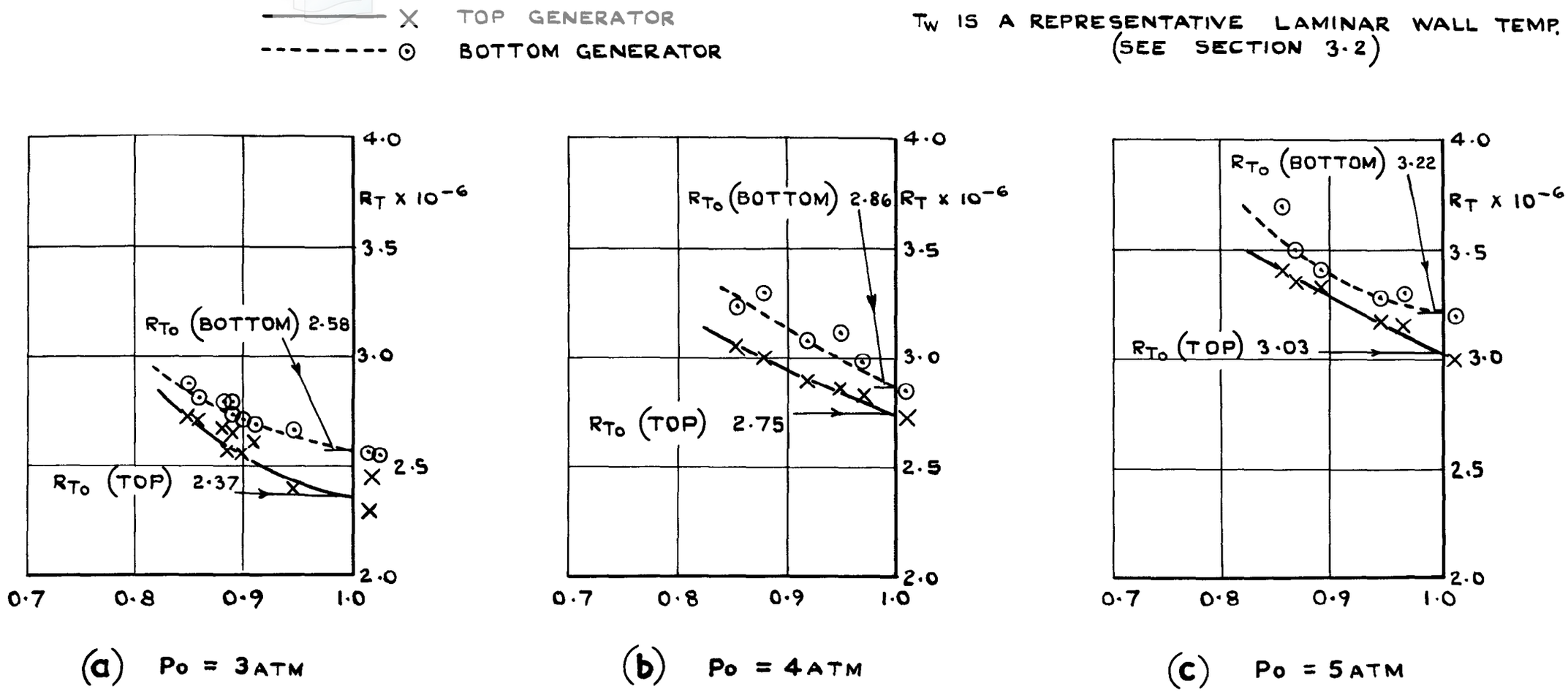

FIG. 7. (a, b, & c) EFFECT OF COOLING ON TRANSITION REYNOLDS NUMBER (FROM SHADOWGRAPH) AT $M_\infty = 3·8$, ($M_1 = 3·48$), AND $P_o = 3-5$ ATM. (ZERO INCIDENCE).

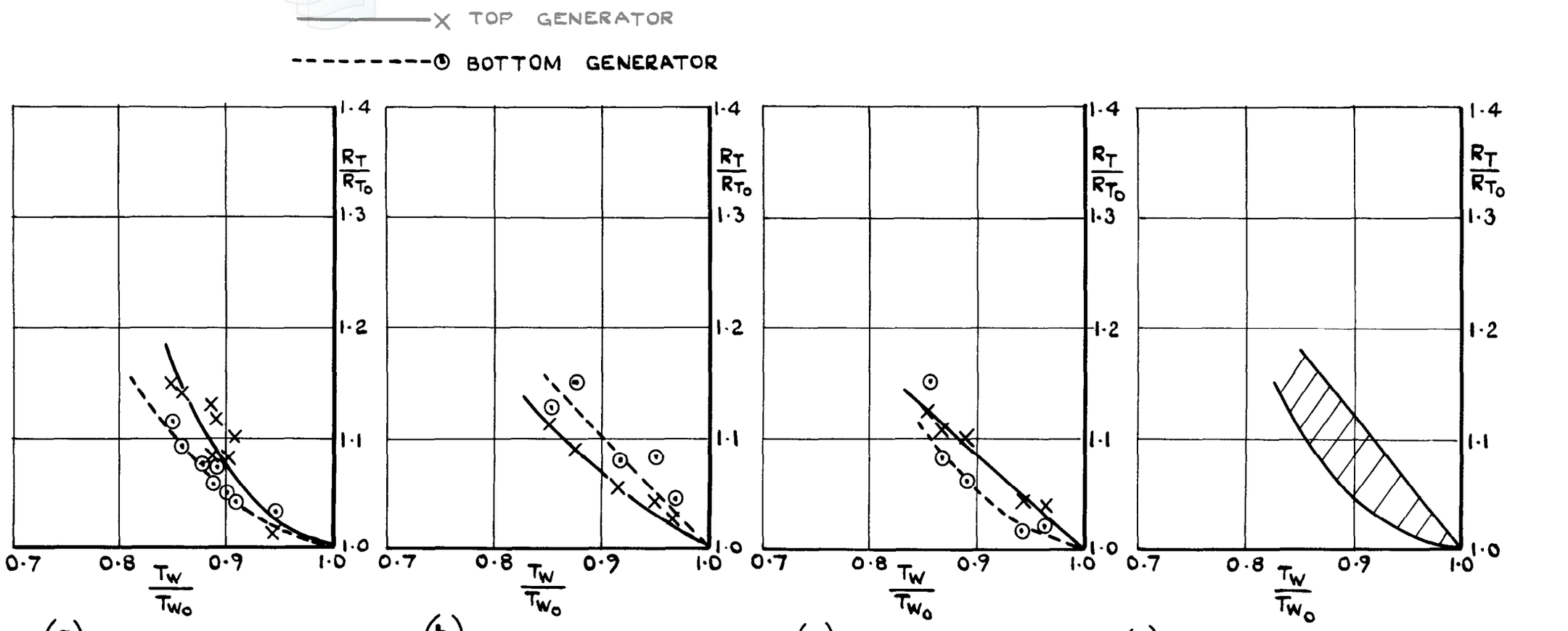

FIG. 8. (a b c & d) EFFECT OF COOLING ON TRANSITION REYNOLDS NUMBER (FROM SHADOWGRAPH) AT $M_\infty = 3{\cdot}8$, ($M_1 = 3{\cdot}48$), AND $P_0 = 3-5$ ATM. (ZERO INCIDENCE)
(R_{T_0} VALUES BEING THOSE INDICATED IN FIG. 7.)

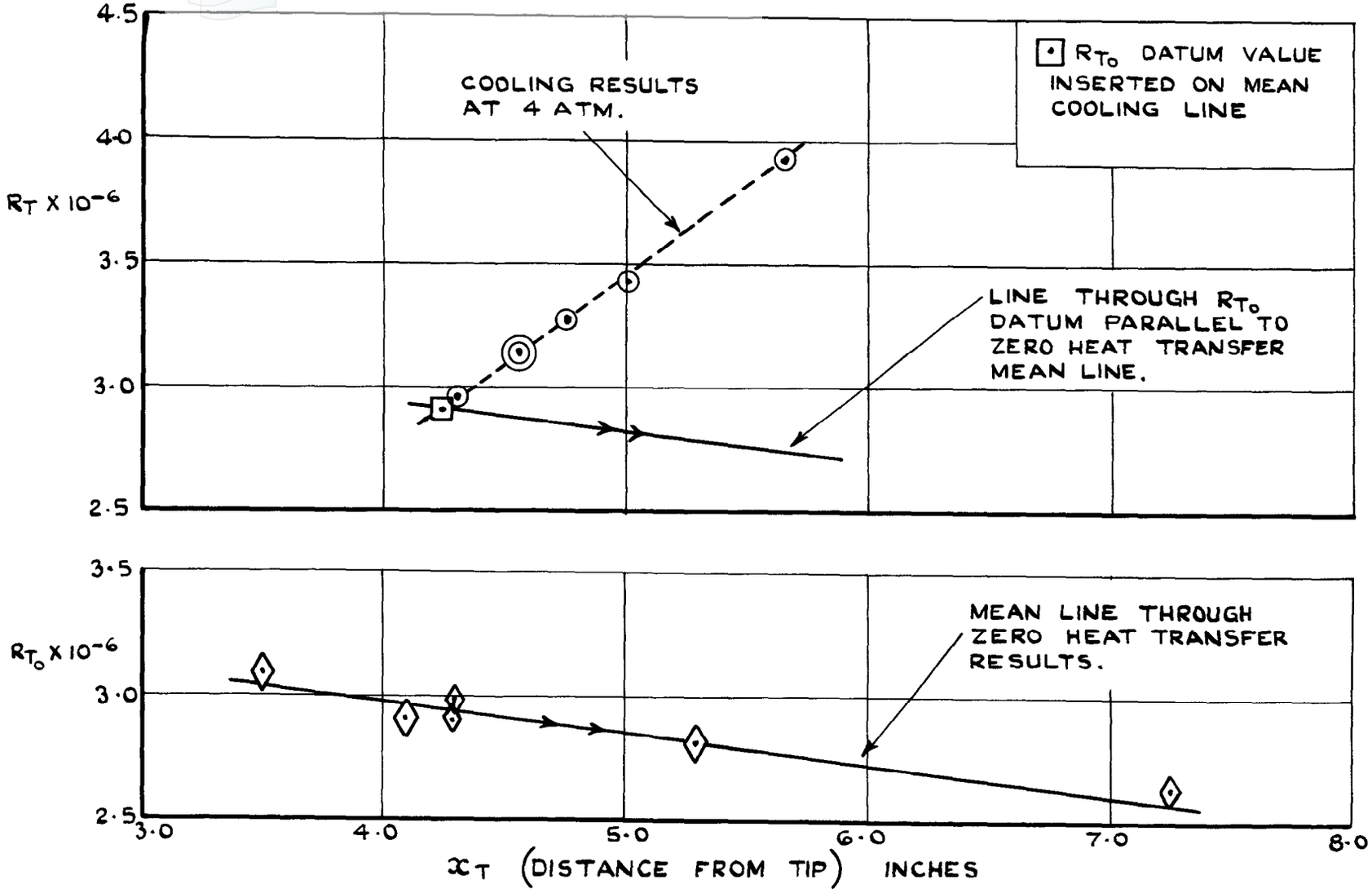

FIG. 9. TRANSITION REYNOLDS NUMBERS OBTAINED AT DIFFERENT DISTANCES FROM THE TIP (x_T) ON THE BOTTOM GENERATOR OF THE CONE AT $M_\infty = 3{\cdot}13$.

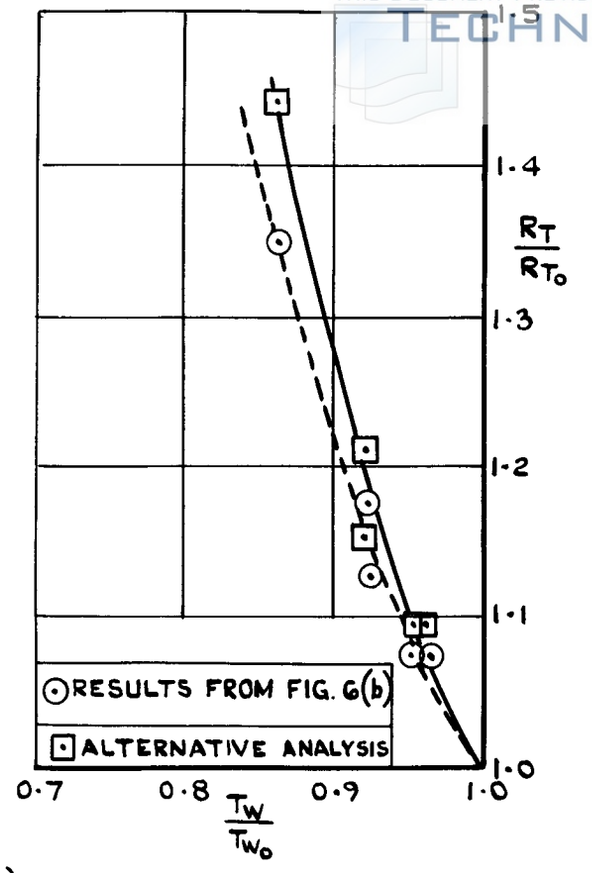

(a) COMPARISON OF THE TWO METHODS OF ANALYSIS FOR THE RESULTS ON THE BOTTOM GENERATOR OF THE CONE AT 4 atm & $M_\infty = 3 \cdot 13$ $(M_1 = 2 \cdot 93)$

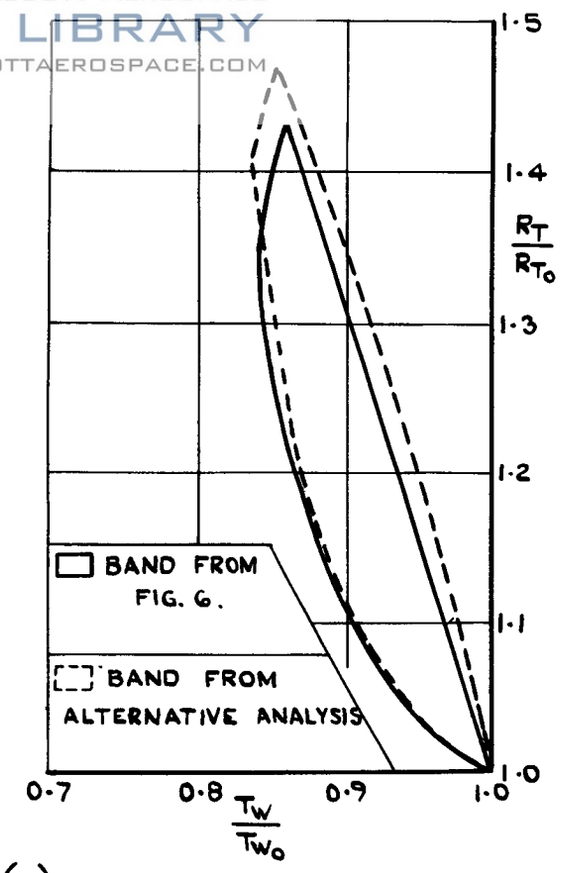

(b) EFFECT OF ALTERNATIVE ANALYSIS ON THE BAND OF COOLING RESULTS AT $M_\infty = 3 \cdot 13$ $(M_1 = 2 \cdot 93)$

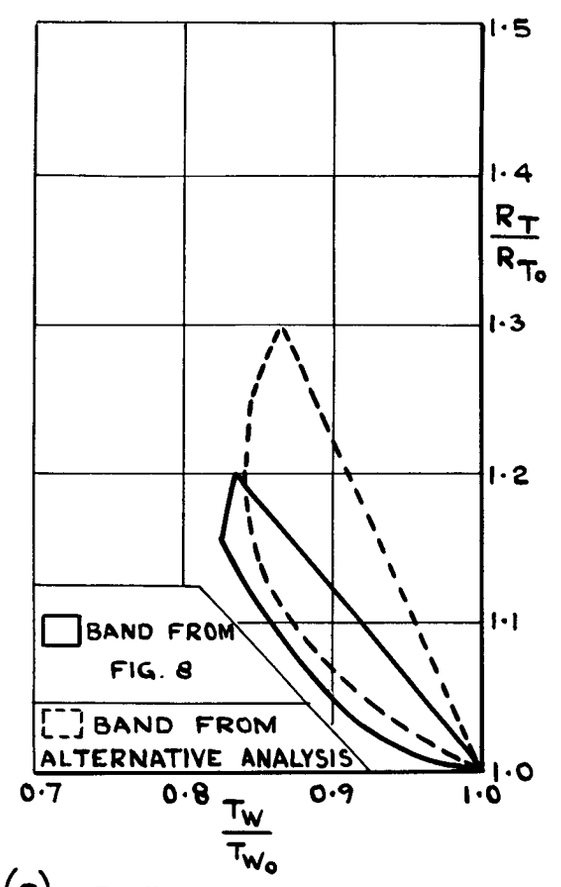

(c) EFFECT OF ALTERNATIVE ANALYSIS ON THE BAND OF COOLING RESULTS AT $M_\infty = 3 \cdot 8$ $(M_1 = 3 \cdot 48)$

FIG. 10. (a, b, & c.) ALTERNATIVE ANALYSIS OF TRANSITION RESULTS WITH COOLING AT M = 3 AND M = 4. (ZERO INCIDENCE.)

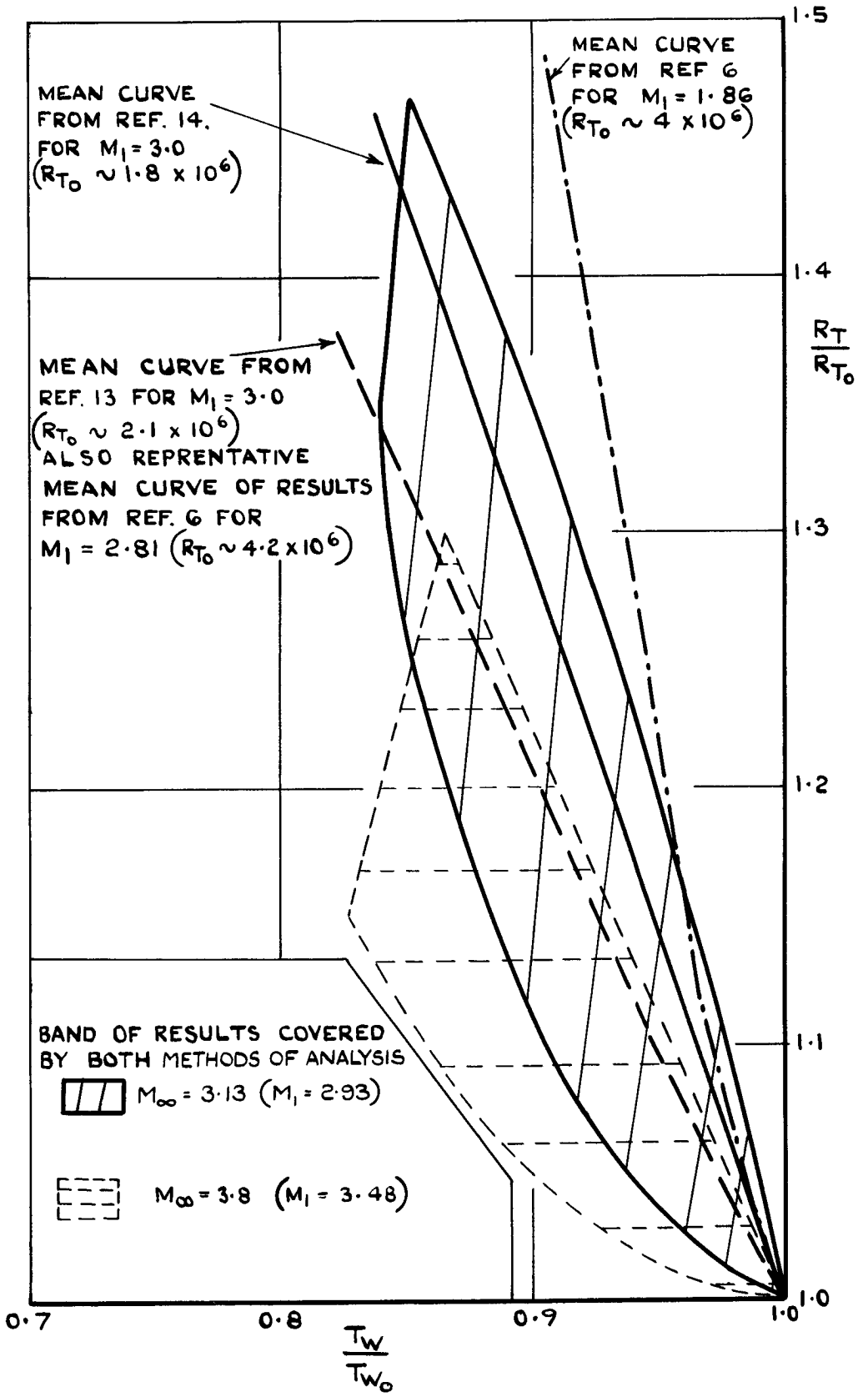

FIG. 11. EFFECT OF LOCAL MACH NUMBER (M_1) ON TRANSITION REYNOLDS NUMBER WITH COOLING ON A CONE AT ZERO INCIDENCE.

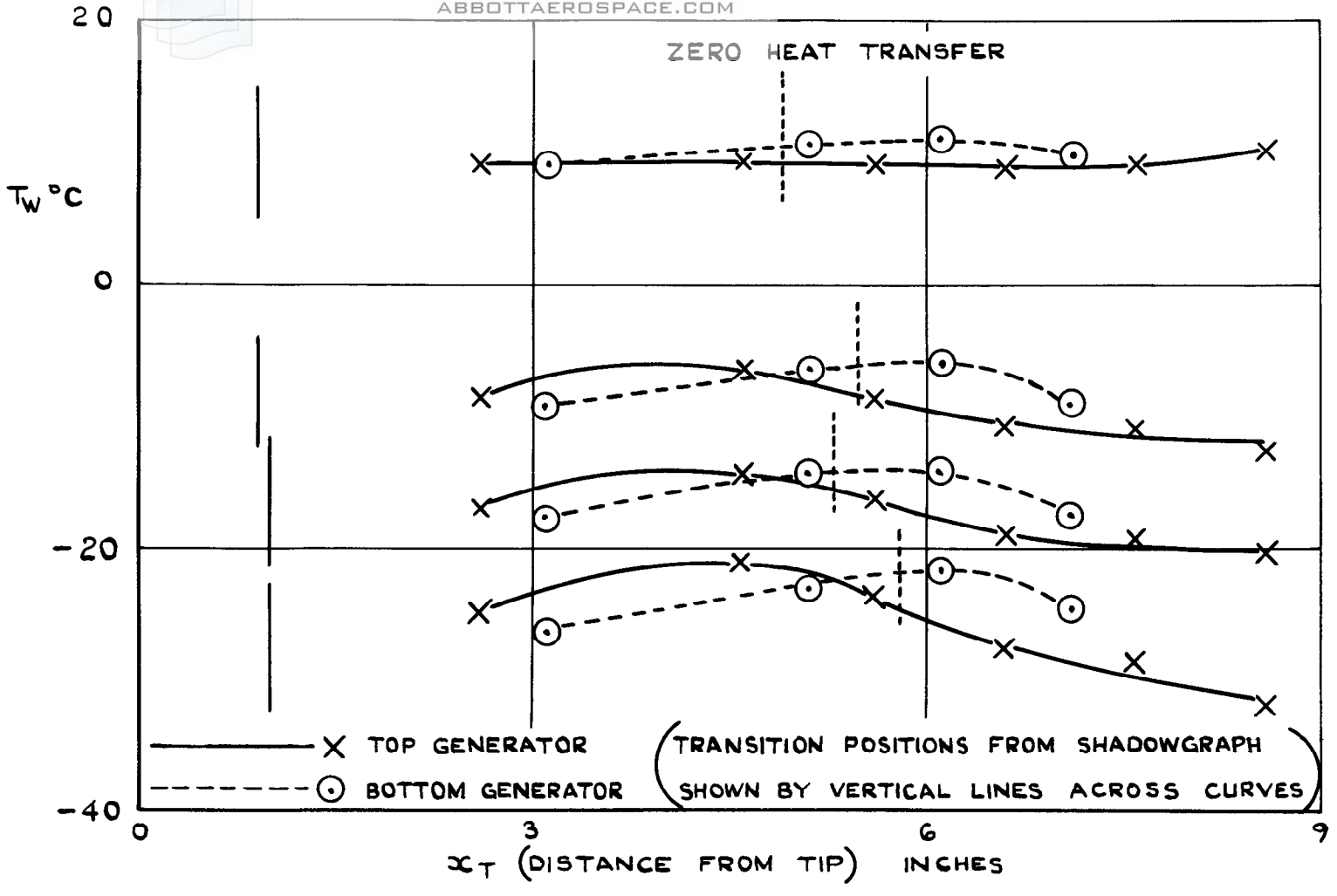

FIG. 12. TYPICAL DISTRIBUTION OF SURFACE TEMPERATURE ALONG THE 15° STEEL CONE AT +2° INCIDENCE FOR $M_\infty = 3.13$ AND $P_0 = 5$ ATM (COOLANT FLOWING FROM BASE TO TIP.)

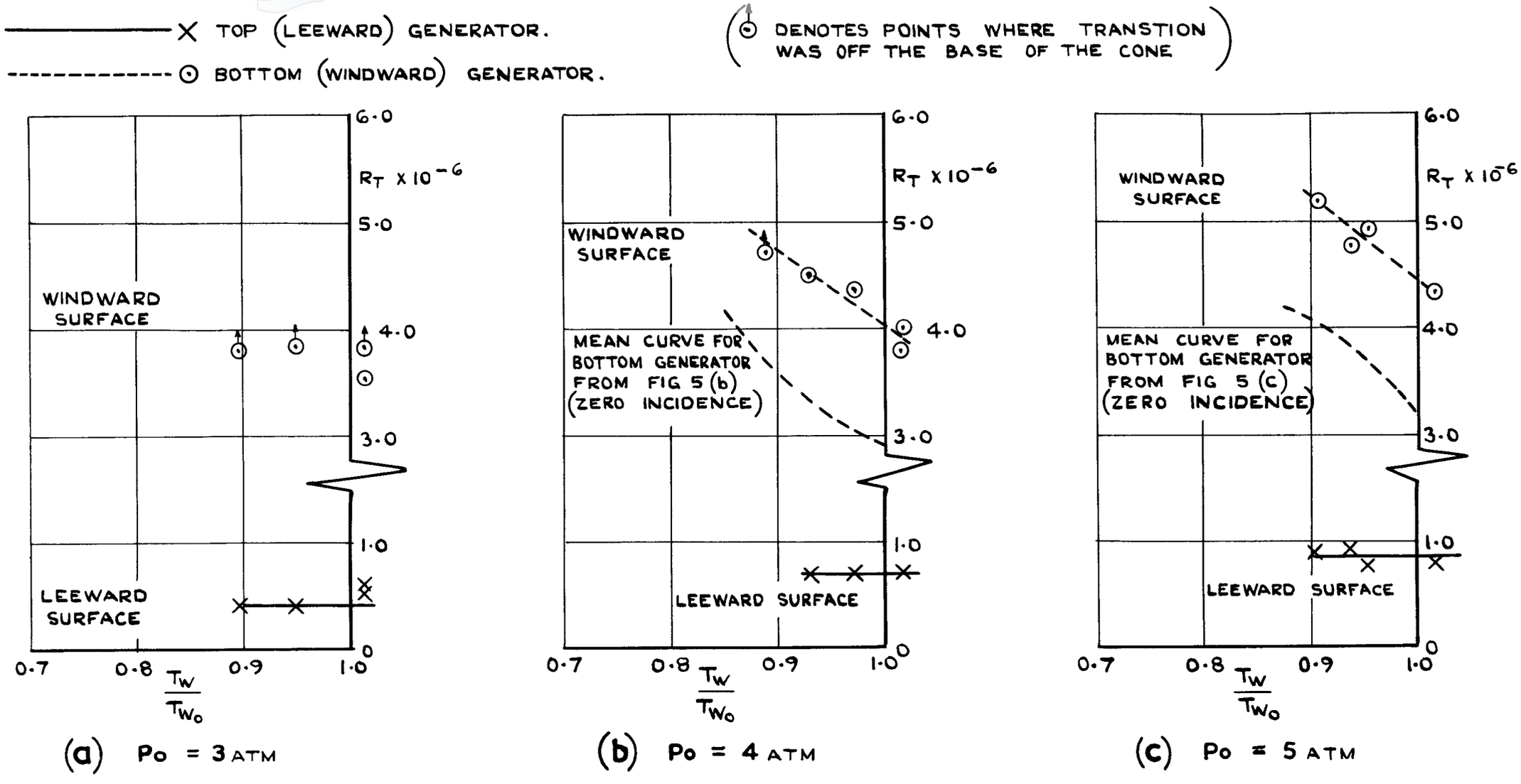

FIG. 13. (a, b, & c) EFFECT OF 2° POSITIVE INCIDENCE ON MOVEMENT WITH COOLING OF TRANSITION POSITION ON A 15° CONE AT $M_\infty = 3{\cdot}13$ (FROM SHADOWGRAPH)

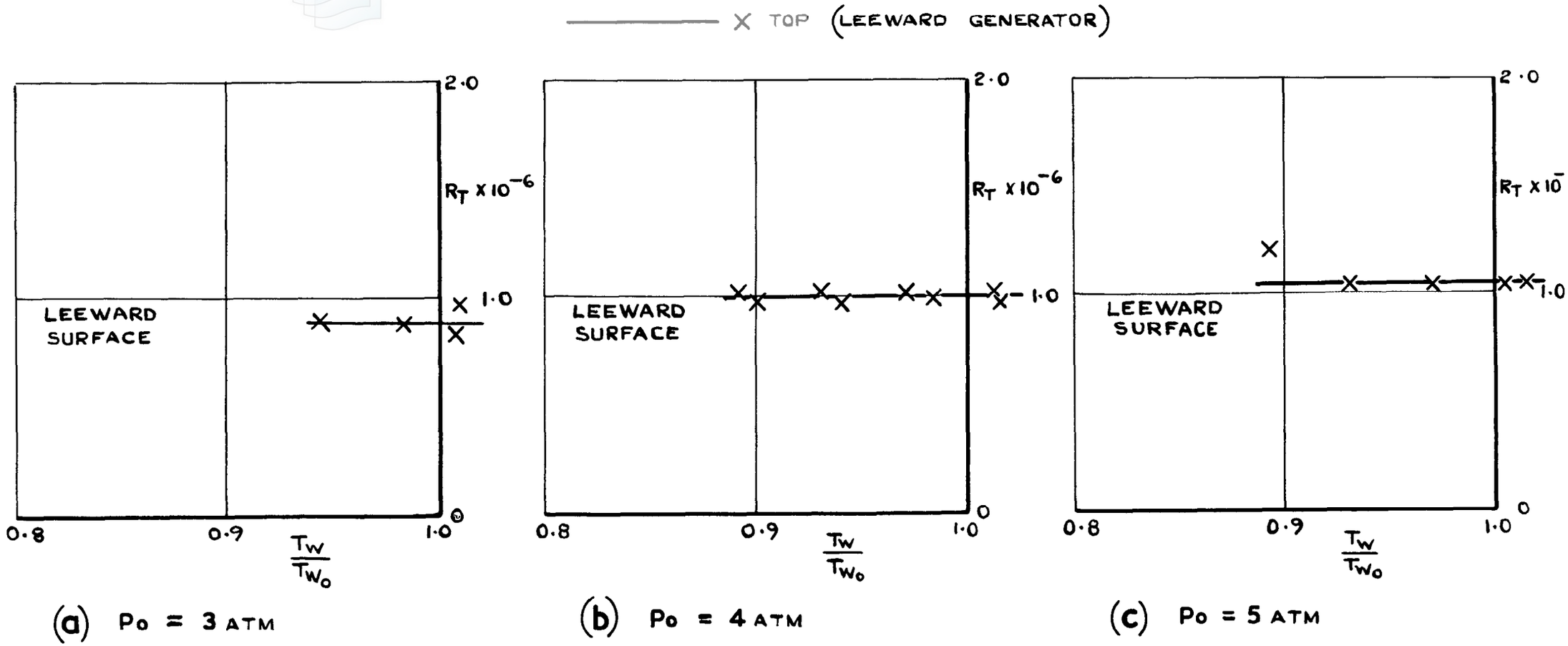

FIG. 14. (a, b, & c) EFFECT OF 2° POSITIVE INCIDENCE ON MOVEMENT WITH COOLING OF TRANSITION POSITION ON THE LEEWARD GENERATOR OF A 15° CONE AT $M_\infty = 3 \cdot 8$ (TRANSITION DID NOT OCCUR ON THE WINDWARD GENERATOR AT THESE PRESSURES.) (FROM SHADOWGRAPH.)

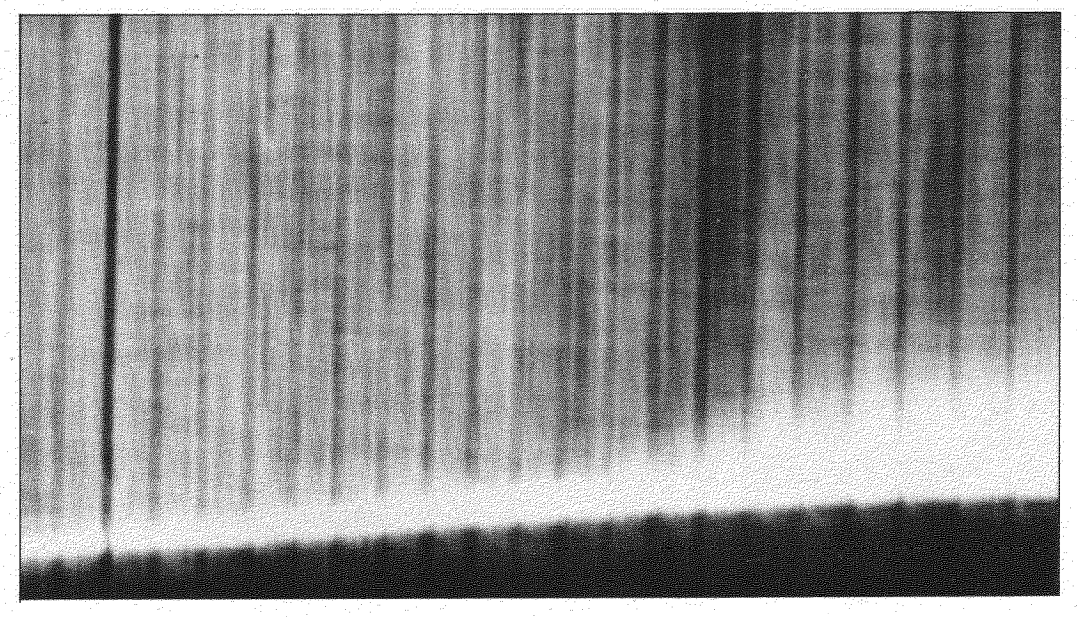

FIG.15. MAGNIFIED SCHLIEREN PICTURE OF THE TRANSITION REGION

(VERTICAL MAGNIFICATION 12:1)

C.P. No. 479
(21,388)
A.R.C. Technical Report

Published by
HER MAJESTY'S STATIONERY OFFICE

To be purchased from
York House, Kingsway, London w.c.2
423 Oxford Street, London w.1
13A Castle Street, Edinburgh 2
109 St. Mary Street, Cardiff
39 King Street, Manchester 2
Tower Lane, Bristol 1
2 Edmund Street, Birmingham 3
80 Chichester Street, Belfast
or through any bookseller

Printed in England

S.O. Code No. 23-9011-79

C.P. No. 479